博士論文

Region- and Cell-specific Expression of Secretory Mucins MUC5AC and MUC5B in Normal Human Airways

(正常ヒト気道における分泌型ムチン MUC5AC と MUC5B の領域および細胞特異的発現について)

奥田　謙一

論文タイトル:

Region- and Cell-specific Expression of Secretory Mucins MUC5AC and MUC5B in Normal Human Airways

(正常ヒト気道における分泌型ムチン MUC5AC と MUC5B の領域および細胞特異的発現について)

所属: 医学系研究科内科学専攻

指導教員名: 長瀬　隆英　教授

申請者名: 奥田　謙一

Table of Contents

1. Abstract

Mucin secretion is a key component of the mucociliary clearance. MUC5AC and MUC5B are the predominant gel-forming mucins in the mucus layer of human airways. However, a systematic study of the site- and cell-specific expression of each mucin in the normal human airways is not available.

To characterize the regional distribution of MUC5AC and MUC5B in normal human airways and assess which cell types produce these mucins, referenced to the club cell secretory protein (CCSP). Multiple airway regions from 16 non-smoker lungs without a history of lung disease were studied. MUC5AC, MUC5B, and CCSP expression/co-localization were assessed by RNA *in situ* hybridization (ISH) and immunohistochemistry in 5 lungs with histologically normal airways. Droplet digital PCR and cell culture were performed for absolute quantification of MUC5AC/5B ratios and protein secretion, respectively.

Our study showed that MUC5B was extensively expressed in submucosal glands as well as superficial epithelia throughout the airways except for the terminal bronchioles. Morphometric calculations revealed that the distal airway superficial epithelium was the predominant site for MUC5B expression, whereas MUC5AC expression was concentrated in proximal, cartilaginous airways. RNA ISH revealed both MUC5B and MUC5AC were colocalized in CCSP+ cells in proximal superficial epithelium, whereas MUC5B was co-localized in CCSP+ cells of distal airway superficial epithelia.

In conclusion, in normal human airways, MUC5B is the dominant secretory mucin in the superficial epithelia as well as glands, with distal airways being a major site of expression. MUC5B and MUC5AC expression is a property of CCSP positive secretory cells in superficial airway epithelia.

Keywords: Airway mucins, MUC5AC, MUC5B, Club cells, Distal airways

2. Abbreviations:

AB-PAS: alcian blue and periodic acid-Schiff

ALI: air-liquid interface

ASL: airway surface liquid

BM: basement membrane

Cas9: CRISPR-associated protein 9

CCSP: club cell secretory protein

CF: cystic fibrosis

CFTR: cystic fibrosis transmembrane conductance regulator

CRISPR: clustered regularly interspaced short palindromic repeats

ddPCR: droplet digital PCR

FOXA3: forkhead box A3

GMH: goblet cell metaplasia and/or hyperplasia

COPD: chronic obstructive pulmonary disease

GAPDH: glyceraldehyde-3-phosphate dehydrogenase

H&E: hematoxylin and eosin

IPF: idiopathic pulmonary fibrosis

ISH: *in situ* hybridization

LAE: large airway epithelial

MCC: mucociliary clearance

NKX2-1: NK2 homeobox1

OBB: odyssey blocking buffer

PBS: phosphate-buffered saline

PBST: phosphate-buffered saline with Tween 20

PCL: periciliary layer

qPCR: quantitative PCR

SAE: small airway epithelial

SFTPB: surfactant protein B

SMG: submucosal glands

UNC: University of North Carolina

3. Introduction

We inhale about 10,000 L of air to take oxygen into our bodies every day. Along with the inhaled air, numerous pathogens, chemical pollutants, and other irritants, which present potential life-threatening risks, are inhaled. A critical innate defense system to maintain lung health is mucociliary clearance (MCC). MCC is dependent on the coordination of three cellular activities in the airway epithelium: 1) appropriate rates of mucin secretion; 2) regulated ciliary beating; and 3) mucus hydration, regulated by transepithelial ion and fluid secretion, which is dependent upon normal cystic fibrosis transmembrane conductance regulator (CFTR) functions (1). Failure of normal MCC results in chronic lung diseases, including CF (2, 3), chronic bronchitis (4), and asthma (5, 6). Especially in CF, an abnormal dehydration of airway surface liquid (ASL) due to absent CFTR function, leading high concentration of mucus, results in slowing of mucus clearance and adhesion of mucus to airway surfaces. Eventually, mucus plugs are generated, followed by persistent bacterial infection and chronic inflammatory changes in the airway, which ultimately lead to patient death. Failed mucus clearance is a common feature of muco-obstructive lung diseases, yet how abnormalities in mucus properties produce intrapulmonary mucus accumulation remains unclear. Part of this uncertainty relates to the absence of a comprehensive formulation that describes all elements of mucus transport in health.

From the biophysical point of view, the structure of ASL has been described with a

two-gel model. This model defines the mucus transport system in mammalian airways as consisting of two airway surface hydrogels (7): 1) a mucus layer composed primarily of the polymeric gel-forming mucins MUC5AC and MUC5B; and 2) a periciliary layer (PCL) composed of tethered mucins such as MUC1, MUC4, MUC16, and MUC20 (8). Notably, this model highlights an important role of mucus concentration that generates partial osmotic pressures that govern water distribution between the two layers. The PCL gel must be well hydrated to facilitate low friction transport of the mucus layer over the PCL (9). Studies of adult CF subjects have identified increased mucus concentration and proportionally raised osmotic pressures in the mucus layer in ranges predicted to slow MCC in CF relative to normal subjects (10).

MUC5AC and MUC5B are the predominant gel-forming mucins in human airways (8, 11-13). The classic paradigm describes MUC5AC secretion in human airways as a feature of superficial epithelial goblet cells whereas MUC5B is predominantly secreted from submucosal glands (SMG) (3, 6, 12, 14, 15). However, previous data generated from mice have demonstrated that the superficial epithelial secretory club cells in large and small airways produce Muc5b, which is rapidly secreted in the absence of alcian blue and periodic acid-Schiff (AB-PAS)-definable mucin granules or goblet cell morphology (16-20). Moreover, studies with Muc5b knockout mice demonstrated that Muc5b is required for normal lung defense and MCC (21), despite the fact that SMG in the mice are restricted to the proximal trachea (22).

Recent studies of normal and diseased human lungs suggest the murine paradigm may also be pertinent to the human lung. In human airways, there are structural and biological differences between proximal large and distal small airways, such as the composition of the cell types lining the airway epithelium and existence of cartilage and submucosal glands, that will influence the expression of the two mucins. Small airways are anatomically distinct from cartilaginous large airways that contain submucosal glands. Generally, there are few goblet cells lining the small airway epithelium, and, it is possible that a majority of the MUC5B in the larger airways is secreted from submucosal glands. However, this cannot be the case in the small airways, which lack submucosal glands. Most muco-obstructive diseases, *e.g.*, CF and COPD, are associated with small airway mucus plugs that are composed of MUC5B as well as MUC5AC (2, 10, 23), suggesting distal airway superficial epithelia may locally secrete the MUC5B associated with plugging (5, 24, 25). Of particular relevance to small airway MUC5B expression is the discovery of the link between MUC5B overexpression in peripheral airways and idiopathic pulmonary fibrosis (IPF) (26, 27).

MUC5AC, on the other hand, is now recognized as a "responsive" mucin with expression known to be regulated by a large number of inflammatory stimuli that are present in the disease environment, including a wide variety of cytokine and growth factor mediators (Th1, Th2, Th17, EGR) and stressors (bacterial and viral infection, smoking, ventilation) (5, 16, 28, 29). The highly responsive nature of MUC5AC suggests that it provides critical innate

immune functions during airway stress.

These findings led us to perform a comprehensive study of region- and cell-specific expression of MUC5B and MUC5AC with an emphasis on comparisons of large airways with superficial epithelia and SMG versus small airways lined exclusively with superficial epithelia. To achieve this aim, multiple complementary approaches, including RNA *in situ* hybridization (ISH), immunohistochemistry, droplet digital PCR (ddPCR) quantification, and primary cell cultures, were utilized to quantitate the regional distribution of MUC5B and MUC5AC expression along the proximal-distal axis of the normal human lung. Based on murine data (17-21), we also explored the hypothesis that club cell secretory protein (CCSP) [also termed secretoglobin 1A member 1 (SCGB1A1)]-expressing secretory cells produce MUC5B, as well as MUC5AC, in human superficial airway epithelia. Some of the results of this study have been previously reported (30).

4. Methods

Subjects and tissue collection.

Human airways were obtained from the University of North Carolina (UNC) Tissue and Cell Culture Procurement Core from transplant donors with lungs unsuitable for transplant due to physical mismatching or poor gas exchange (31). Inclusion criteria were developed to define normal lung samples used for the study (below). Our studies were performed in lungs from both sexes. Human lung tissue was procured under the UNC Office of Research Ethics Biomedical Institutional Review Board-approved protocol No. 03-1396. Our studies used human airways resected from a total of 16 normal lung samples obtained consecutively from May 2016 to March 2018. The demographics of the subjects studied are shown in Table 1. All subjects were without history of chronic lung disease. Fifteen of the 16 subjects were lifetime non-smokers and one subject (#12 in Table 1) had a 2 pack-year smoking history but had quit smoking 30 years previously. *MUC5B* promoter variant rs35705950 genotypes were determined using TaqMan (Life Technologies) genotyping (32).

Inclusion criteria to define normal lung samples:

- The tissues were obtained from transplant donors with lungs unsuitable for lung transplantation.
- The donors must be 15 years old or older.
- No current smokers.

- Free of known history of chronic lung diseases before admission.
- The lung must have been subjected to mechanical ventilation for less than 7 days.
- The lung must have been transferred to the UNC Core within 36 hours of surgical resection.

Table 1: Subject demographics and experimental use.

#	Age (years)	Sex	Ventilation period (days)	*MUC5B* promoter variant rs35705950 genotype	Morphometric studies		Cell culture	ddPCR
					H&E AB-PAS	RNA ISH IHC		
1	43	M	1	G/G	X	X		
2	17	F	3	G/G	X	X	X	
3	36	F	6	G/G	X	X	X	
4	22	F	1	G/G	X	X		
5	55	F	1	G/G	X	X		
6	19	F	3	G/G	X			
7	37	M	1	G/G	X		X	
8	67	F	6	G/G	X			
9	28	M	1	G/G	X			
10	57	F	1	G/G	X			
11	55	M	1	G/G			X	X
12	53	F	3	G/G				X
13	24	M	1	G/G				X
14	59	F	3	G/G				X
15	25	M	1	G/G				X
16	15	M	2	G/T				X

Abbreviations: RNA ISH = RNA *in situ* hybridization; IHC = immunohistochemistry: ddPCR = droplet digital PCR.

Subjects and tissues for RNA ISH and immunohistochemistry studies of MUC5AC, MUC5B, and CCSP localization in histologically normal human lungs.

Lungs obtained from 10 amongst the 16 normal subjects studied were used for initial experiments to evaluate MUC5AC, MUC5B, and CCSP mRNA and protein localization by RNA ISH and immunohistochemistry. After transportation of the experimental lung to the UNC Tissue and Cell Culture Core, the excised lung was dissected to obtain defined airway regions, including tracheas, primary bronchi, and segmental bronchi (Figure 1). Lung parenchyma potentially containing distal bronchi and/or bronchioles was obtained from 2 to 8 blocks per lung (depending on tissue availability), whose locations were chosen randomly. Each dissected lung tissue specimen was fixed in 10% neutral buffered formalin for 24-36 hours followed by paraffin-embedding. The paraffin blocks were cut to produce 5 μm serial sections for H&E and AB-PAS staining.

Figure 1

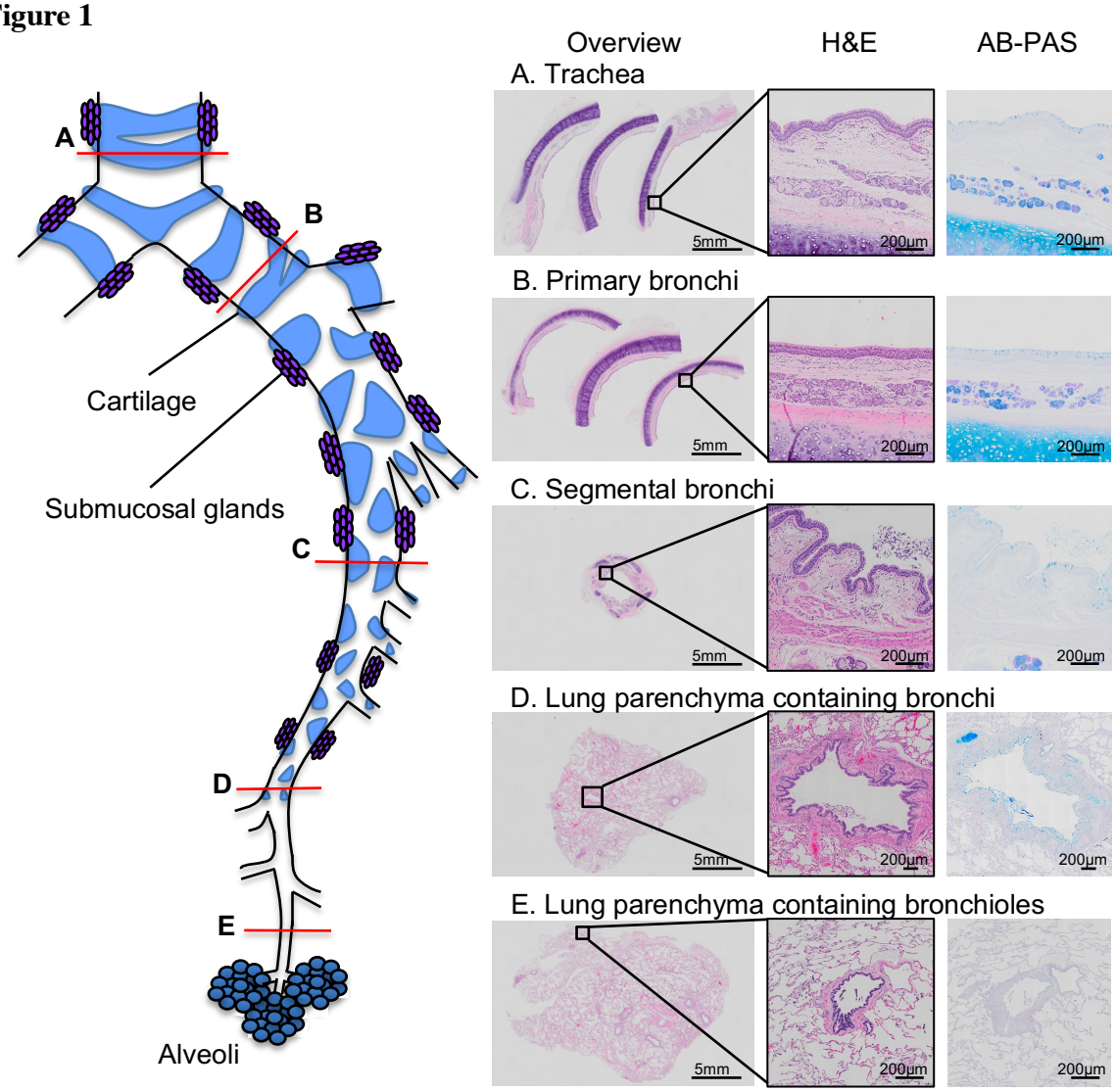

Figure 1. Overview of the airway tissue sections utilized in this study. The excised lung was dissected at different levels to obtain: (A) trachea; (B) primary bronchi; (C) segmental bronchi; and (D, E) lung parenchyma containing distal bronchi and bronchioles. H&E: hematoxylin and eosin. Alcian blue and periodic acid-Schiff (AB-PAS) stains for mucous glycoproteins.

Since mechanical ventilation has been shown to acutely induce airway goblet cell metaplasia and/or hyperplasia (GMH) in normal animals/humans (28, 33-36), a protocol was devised to identify histologically normal lungs. Ten lungs were assessed histologically by H&E and AB-PAS staining to evaluate features of normalcy. The tissues were defined as histologically normal by a pathologist when the tissues did not meet any of the exclusion criteria listed below. These exclusion criteria were established using a modification of the previously reported method (37, 38). Since the mean value of AB-PAS-stained volume densities in primary bronchial epithelium in healthy subjects based on bronchoscopic biopsy samples was reported as 0.005 mm^3/mm^2 in a previous study (37), consistent with a similar report (39), we utilized 0.005 mm^3/mm^2 as the cut-off value to distinguish airways with GMH from histologically normal airways without GMH. We included lungs for study with moderate neutrophil infiltration in the trachea as long as such neutrophil infiltration was considered to be the effect of tracheal intubation.

Exclusion criteria to define histologically normal lung samples based on H&E and AB-PAS staining:

- Goblet cell metaplasia and/or hyperplasia.
- Squamous cell metaplasia.
- Smooth muscle hypertrophy in the airway walls.
- Severe inflammatory cell infiltration within airway epithelium.

Amongst the 10 subjects, one or more airway regions with GMH were identified in five subjects and these five subjects were excluded from further studies by RNA ISH and immunohistochemistry. Squamous cell metaplasia, smooth muscle hypertrophy in the airway walls, or severe inflammatory cell infiltration within airway epithelium were not identified in these 10 subjects. Accordingly, lungs obtained from the five subjects without airway GMH were selected as histologically normal lungs for the further study. Serial sections were used for RNA ISH and immunohistochemistry.

Subjects and tissues for ddPCR to quantitate *MUC5AC* and *MUC5B* transcript copy numbers in freshly isolated normal human airway epithelia.

For absolute quantification of *MUC5AC* and *MUC5B* transcript copy numbers by ddPCR in different regions of human airways, including tracheas, segmental bronchi, bronchioles and peripheral lung parenchyma, tissues were obtained from 6 normal subject donors amongst the 16 subjects studied (Table 1). Since we particularly focused on the examination of *MUC5AC* and *MUC5B* transcript copy numbers in histologically normal distal airways, histological evaluations of the lungs were performed by H&E and AB-PAS staining. Importantly, none of the exclusion criteria (see above) were demonstrated in bronchioles in the 6 subjects. For ddPCR samples, epithelial cells were physically scraped with a knife from a piece of the trachea and longitudinally-opened segmental bronchi to exclude submucosal

glands, followed by centrifugation (2000 rpm, 5 min, 4 °C) (10). The isolated epithelial cells were suspended in 1 ml of TRI Reagent (Sigma), debris was pelleted by centrifugation, and the supernatant was used for RNA analysis. Dissected small airways and peripheral lung parenchyma were homogenized in 1 ml of TRI Reagent using a tissue homogenizer (Bertin Technologies) and then centrifuged (2000 rpm, 5 min, 4 °C). The supernatant was used for RNA analysis.

Subjects for large and small airway epithelial cell culture.

Matched large airway epithelial (LAE) and small airway epithelial (SAE) cells were isolated from 4 of the 16 normal subjects studied (Table 1). Isolated LAE and SAE cells were separately expanded using a modified conditional reprogramming cell method (40, 41), and then grown to obtain well-differentiated air-liquid interface (ALI) cultures. Since we particularly attempted to investigate MUC5AC and MUC5B protein expression in histologically normal distal airways, histopathological examinations of the lungs used to generate these cultures were performed by H&E and AB-PAS staining. Importantly, none of the exclusion criteria (see above) were determined in bronchioles in the 4 subjects.

Immunohistochemistry.

Immunohistochemical staining was performed for MUC5AC, MUC5B, CCSP and

FOXA3 proteins. Briefly, paraffin-embedded sections were baked at 60 °C for 2–4 hours, and deparaffinized with xylene (2 changes × 5 min) and graded ethanol (100% 2 × 5 min, 95% 1 × 5 min, 70% 1 × 5 min). After rehydration, antigen retrieval was performed by boiling the slides in 0.1 M sodium citrate pH 6.0 (3 cycles with microwave settings: 100% power for 6.5 min, 60% for 6 min, and 60% for 6 min, refilling the Coplin jars with distilled water after each cycle). After cooling and rinsing with distilled water, quenching of endogenous peroxidase was performed with 0.5% hydrogen peroxide in methanol for 15 min, slides washed in phosphate-buffered saline (PBS), and blocked with 4% normal donkey serum, for an hour at room temperature. Primary antibodies and isotype control antibodies (mouse gamma globulin, 1:1000, chrome pure rabbit IgG, 1:500, Jackson ImmunoResearch, and goat IgG, 1:250, Invitrogen) were diluted in 4% normal donkey serum in PBS with Tween 20 (PBST) (Fisher Scientific) and incubated over night at 4 °C. Primary antibodies used for immunohistochemistry are described in Table 2. Sections were washed in PBST and secondary antibodies (biotinylated donkey anti-rabbit IgG, biotinylated goat anti-mouse IgG and biotinylated mouse anti-goat IgG Jackson ImmunoResearch, at 1:200 dilution in 4% normal donkey serum in PBST) were applied for 60 min at room temperature. After washing in PBST, slides were incubated with avidin-peroxidase complex according to the manufacturer's instructions (Vectastain kit, Vector laboratories), washed, incubated with the chromogenic substrate (Immpact Novared, Vector laboratories) and counterstained with Fast Red.

Coverslipped slides were scanned and digitized using an Olympus VS120 slide scanner light microscope with a 40X 0.95 NA objective.

Table 2: Antibodies used for immunohistochemistry

Target	Company, Catalog No.	Dilution	2nd antibody
MUC5B	Santa Cruz, H300, sc-20119	1:500	Donkey α-Rabbit
MUC5AC	Abcam, 45M1, ab3649	1:1000	Goat α-Mouse
CC10 (CCSP)	Santa Cruz, E11, sc-365992	1:1000	Goat α-Mouse
FOXA3	Santa Cruz, N19, sc-5361	1:250	Mouse α-Goat

RNA *in situ* hybridization (ISH).

RNA ISH was performed on paraffin-embedded 5 μm tissue sections using an RNAscope 2.5 HD Reagent Kit, RNAscope 2.5 HD Duplex Reagent Kit and RNAscope Multiplex Fluorescent Assay v2, according to the manufacturer's instructions (Advanced Cell Diagnostics). Briefly, tissue sections were deparaffinized with xylene (2 changes × 5 min) and 100% ethanol (2 changes × 1 min), and then incubated with hydrogen peroxide for 10 min, followed by target retrieval in boiled water for 15 min, and protease plus (Advanced Cell Diagnostics) for 15 min at 40 °C. Slides were then hybridized with custom probes, *i.e.*, Hs-*MUC5AC* (#449881), Hs-*MUC5B* (#312891), Hs-*CCSP* (#469971), and Hs-*SFTPB* (#544251) in the HybEZ oven (Advanced Cell Diagnosis) at 40 °C for 2 hours. Target regions of each RNAscope probe are described in Table 2. The Hs-*UBC* probe for the human housekeeping gene *UBC* was used as a control to test for RNA quality. The bacterial gene *DapB* was used as

a negative control (Figure 2). After hybridization, slides were subjected to signal amplification according to the manufacturer's instructions. Hybridization signals were detected using a mixture of solutions A and B (1:60) in RNAscope 2.5 HD Assay RED and RNAscope 2.5 HD Duplex Assays, and Opal 520, 570, and 650 (Perkin Elmer) in RNAscope Multiplex Fluorescent Assay v2. After counterstaining with 50% hematoxylin, slides were dried in a dry oven at 60 °C for 30 min and mounted with VectaMount (Advanced Cell Diagnostics) for RNAscope 2.5 HD Assay RED and RNAscope 2.5 HD Duplex assays. The stained sections were scanned and digitized using an Olympus VS120 light microscope with a 60X 1.35 NA objective. In RNAscope Multiplex Fluorescent Assay v2, after counterstaining with DAPI, glass coverslips were placed over tissue sections with ProLong Gold Antifade Reagent (Thermo Fisher Scientific) and the images were captured using an Olympus confocal microscope with a 20X 0.75 NA, 40X 0.6 NA or 60X 1.4 NA objective. For the sections obtained from LAE and SAE cell culture membrane, the period and temperature for protease incubation were changed to 5 min at room temperature, otherwise, the same protocol was used.

Table 3: Probes used for RNA *in situ* hybridization

Probe Name	Catalog No.	Accession No.	Target Start	Target Stop
Hs-*MUC5B*	449881	NM_002458.2	3599	4698
Hs-*MUC5AC*	312891	XM_003403450.3	761	2125
Hs-*SCGB1A1* (*CCSP*)	469971	NM_003357.4	8	441
Hs-*SFTPB*	544251	NM_000542.3	685	1664

Figure 2

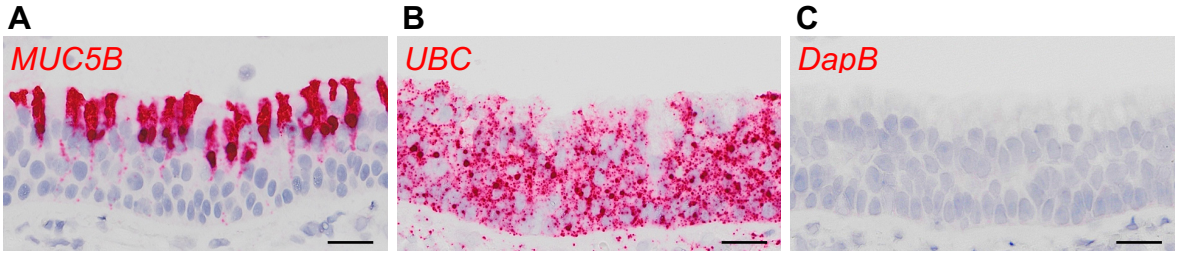

Figure 2. Representative RNA ISH results for target, positive and negative control probes in histologically normal human trachea. A. Representative RNA ISH image for target (*MUC5B*) mRNA. B. The human housekeeping gene *UBC* was used as a positive control. C. The bacterial gene *DapB* was used as a negative control. Scale bars = 25 μm.

Morphometric analysis.

Classification of airways. The airways were classified based on a combination of airway diameter and morphology into: 1) trachea, 2) primary bronchi, 3) segmental bronchi, 4) distal bronchi, 5) proximal bronchioles, 6) distal bronchioles, and 7) terminal bronchioles (42). The airways from trachea to segmental bronchi were dissected and separately fixed in 10% neutral buffered formalin as described above (Figure 1). In the section of lung parenchyma potentially containing distal bronchi and/or bronchioles, airways with cartilage and/or submucosal glands were classified as distal bronchi regardless of the diameter of the airway. The airways with diameters of 2 mm or greater were also defined as distal bronchi even though they did not exhibit cartilage or submucosal glands. Bronchioles were defined as airways that did not have cartilage or submucosal glands and had diameters less than 2 mm. Bronchioles were classified into three categories: proximal bronchioles, *i.e.*, bronchioles with a diameter from 1 mm to 2 mm; distal bronchioles, *i.e.*, bronchioles with diameters smaller than 1 mm

with no direct connection to alveolar space; and terminal bronchioles, *i.e.*, bronchioles which transitioned to respiratory bronchioles where alveolar sacs were present along the bronchiolar wall. We used Fiji (National Institute of Health Image) to determine a diameter of distal bronchi, proximal and distal bronchioles. The diameter (D) of the airway was calculated using the length of basement membrane (BM) and formula $D = BM/\pi$. BM was measured by tracing the image of airway basement membrane using the computer mouse in Fiji.

Quantitation of mucous glycoproteins, MUC5AC, MUC5B, and CCSP in AB-PAS, immunohistochemistry and RNA ISH. All airway sections were scanned and digitized at a magnification 10X for sections stained with AB-PAS, 40X for immunohistochemistry, and 60X for RNA ISH, respectively, using Olympus VS120 slide scanner light microscope. In the trachea, primary and segmental bronchi, images of all the intact epithelium, except for submucosal ducts, in each section were captured from the scanned images to quantify stained volumes. For the more distal airways, all the bronchi and bronchioles contained in each section were analyzed. Images from each of the distal bronchi or three types of bronchioles were individually captured from the scanned images so that an entire airway was included in the field. Only airways cut as the cross section were analyzed. If airways were cut as longitudinal sections or the epithelial layer was disrupted, the airways were excluded from analysis.

Stained volumes for mucous glycoproteins, MUC5AC, MUC5B or CCSP mRNAs and proteins within the airway superficial epithelium, obtained from the results of AB-PAS staining,

RNA ISH or immunohistochemistry, respectively, were quantitated using Fiji by blinded investigators. First, the outside and inside regions of the airway epithelium were isolated from the field to remove staining artifacts and stained intraluminal mucus (Figure 3A, B). Second, the length of BM was measured and used for normalization of stained volumes per the formula below. Third, the image of the target epithelium, which was left after isolating the inside and outside regions of the airway epithelium, was converted to a gray-scale image (Figure 3C), followed by quantification of the areas above the optimized threshold values. We determined the optimized threshold value by adjusting the threshold until the threshold (black and white) image accurately represented the original images. After the optimized threshold value was determined, the same threshold value was applied to the sections stained by either AB-PAS, RNA ISH or immunohistochemistry. The area above the threshold value (A) as shown in Figure 3C was then measured (43). The volume densities of intracellular mucous glycoproteins, MUC5AC, MUC5B or CCSP mRNAs and proteins were calculated as described previously (20, 37, 44, 45). Briefly, the volume density of mucous glycoproteins, MUC5AC, MUC5B or CCSP mRNAs and proteins, was calculated as (A) / [(BM) (4/π)]. As a result, data are presented as the volume of intracellular mucous glycoproteins, MUC5AC, MUC5B or CCSP mRNAs or proteins per unit surface area of the basement membrane.

Figure 3

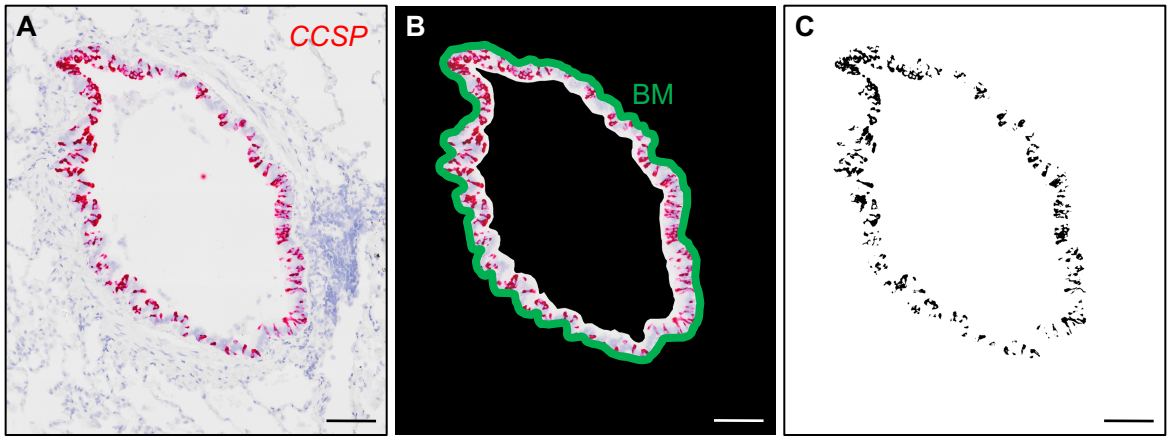

Figure 3. Method for quantification of RNA ISH signals within airway superficial epithelium. Stained volumes for *MUC5AC*, *MUC5B*, and *CCSP* mRNAs within airway superficial epithelia obtained from RNA ISH were morphometrically quantified. A. Representative histologically normal human bronchiole stained for *CCSP* mRNAs (red) by RNA ISH. B. The basement membrane (BM) and airway superficial epithelia were delineated to create a region of interest including exclusively the airway epithelia. C. Stained areas within airway superficial epithelia were converted to a gray-scale image, and the black areas above optimized threshold values were quantified using Fiji (National Institutes of Health Image). Scale bars = 100 μm.

Quantification of region-specific *MUC5B*, *MUC5AC* and *CCSP* mRNAs. To calculate the sites that dominate mucin secretion in the normal lung, we referenced the stereological parameters reported by Weibel et al (46, 47). Each airway generation was assigned to each airway region classified in the current study, adjusting the diameter and anatomical features of airways. The airways which are partially alveolated were classified into terminal bronchioles. Total *MUC5AC*, *MUC5B* or *CCSP* mRNA-stained volumes for each airway region were calculated by multiplying the mean values of the RNA ISH volume densities for each airway region obtained from the five histologically normal lungs by predicted total surface area of corresponding airway regions. The calculated *MUC5B*, *MUC5AC* or *CCSP* mRNA-stained

volumes for each airway region are shown as the percent of total *MUC5B*, *MUC5AC*, or *CCSP* mRNA-stained volumes in airway superficial epithelium of the whole lung (See "Region-specific superficial epithelial mucin production in histologically normal human lungs" in the Results).

Evaluation of co-localization. Co-localization of *MUC5AC*, *MUC5B* and *CCSP* mRNAs was determined using the RNAscope Multiplex Fluorescent Assay v2 (Advanced Cell Diagnostics). Submucosal glands, primary bronchi, distal bronchioles, and terminal bronchioles from the five histologically normal lungs were examined. Three or four fields per airway region were randomly selected and captured at 40X by an Olympus confocal microscope so that the total length of basement membrane of studied epithelium for each airway region exceeded 1 mm. Airway epithelial cells that expressed *MUC5AC*, *MUC5B*, *CCSP* mRNAs, or their combination, were classified into one of the possible 7 types. The number of cells classified into each cell type was manually counted using Fiji and normalized to unit length of corresponding basement membrane. Briefly, we first distinguished *MUC5AC*, *MUC5B* or *CCSP* mRNA positive cells from triple negative cells by manually drawing the cell borders (Figure 4A). Next, by selectively turning on the fluorescent channel for each target gene, we assessed whether *CCSP*, *MUC5B* and/or *MUC5AC* mRNA positive signals were expressed inside the individual cells that were circled with a border (Figure 4B-D). Thereafter, we manually counted the number of cells per each cell type using a cell counter in Fiji (Figure

4E). One or more dot signals and/or clusters designated a positive cell. Staining intensity was not considered when we assessed the positivity of *MUC5AC*, *MUC5B* or *CCSP* mRNA signals in each individual cell since the amplification levels depend on the probe in the RNA ISH multiplex assay.

Figure 4

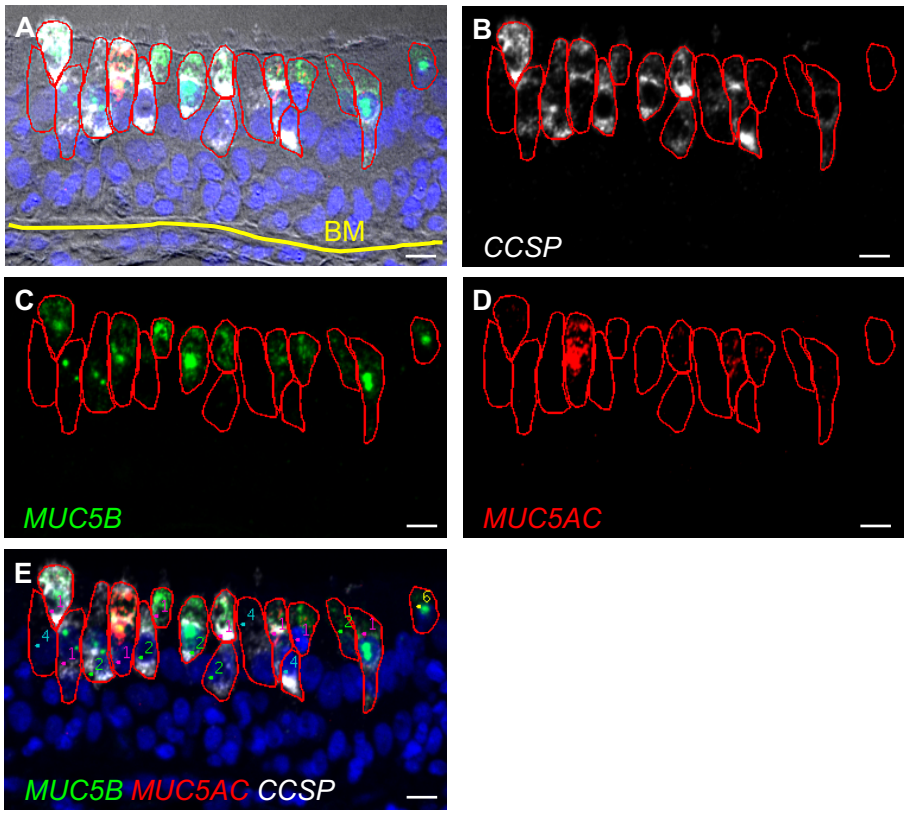

Figure 4. Method for quantitation of co-localization of *MUC5AC*, *MUC5B* and *CCSP* mRNAs in airway epithelium. Co-localization of *MUC5AC* (red), *MUC5B* (green), and *CCSP* (white) mRNAs was performed using RNA ISH. A. Representative histologically normal human primary bronchial epithelium stained for *MUC5AC*, *MUC5B*, and *CCSP* mRNAs by RNA ISH. The fluorescent images were overlaid with differential interference contrast images. Cell borders (red lines) were manually drawn for all *MUC5AC*, *MUC5B* and/or *CCSP* mRNA positive cells to distinguish them from triple negative cells. B-D. *MUC5AC*, *MUC5B* and/or *CCSP* mRNA positive signals were assessed for each individual cell by selectively turning on the fluorescent channel for each target gene. E. The number of cells per each cell type were manually counted using a cell counter in Fiji (National Institutes of Health Image) and normalized to unit length of the basement membrane (BM): (1) *CCSP*+/*MUC5B*+/*MUC5AC*+ cells; (2) *CCSP*+/*MUC5B*+/*MUC5AC*- cells; (4) *CCSP*+/*MUC5B*-/*MUC5AC*- cells; (6) *CCSP*-/*MUC5B*+/*MUC5AC*- cells. Scale bars = 10 μm.

Human large and small airway epithelial cell cultures.

LAE cells were isolated from the larger cartilaginous airways by protease digestion and provided by the UNC Tissue Procurement and Cell Culture Core as previously described (48). For human SAE cell isolation, a piece of distal lung was obtained from the same lungs as dissected for LAE cell isolation (Figure 5). Small airways were identified based on the absence of wall cartilage and outer diameters less than 2 mm. The absence of both cartilage and submucosal glands was retrospectively confirmed by histological examination. The bronchioles were then carefully dissected free from the surrounding lung parenchyma and blood vessels under light microscopy. The branched small bronchioles with alveoli were cut free to avoid being contaminated by lung alveolar epithelial cells. Immediately, dissected small airways were placed in dishes containing F12 medium on ice, and then bronchioles were longitudinally cut. SAE cells were isolated by digestion with 0.5 ml of freshly prepared pronase (10 mg/ml) (Roche) and 5 ml accutase (Sigma) for 2 hours at room temperature. After neutralization of these enzymes by 10% fetal bovine serum, SAE cells were harvested by centrifugation (2000 rpm, 2 min, 4 °C). LAE and SAE cells were co-cultured with mitomycin-treated 3T3 J2 cells on collagen-coated tissue culture plastic dishes in DMEM media supplemented with 10 μM Y-27632 (Enzo Life Science). At 70-90% confluence, LAE and SAE cells were passaged and sub-cultured for expansion. P2 LAE and SAE cells were transferred to human placental type IV collagen-coated, 0.4 μm pore size Millicell inserts (Millipore,

PICM01250). The LAE and SAE cells were seeded at a density of 2.8×10^5 cells/cm^2 and cultured in UNC ALI media (41). Upon confluence, usually at 5-7 days, cells were maintained at an ALI by removing apical media and providing UNC ALI media to the basal compartment only. Medium was replaced in the basal compartment twice a week, and the apical surfaces were washed with PBS once a week. After 21 days in culture, the apical surfaces were washed with PBS to remove accumulated mucus and then maintained without washing for 7 days. After 28 days, the apical surfaces were washed with 200 µl PBS and this solution was frozen at -80 °C for analysis of secreted protein. After washing apical surfaces, LAE and SAE cells were collected for RNA isolation. Other LAE and SAE cells were not washed and were fixed in 4% paraformaldehyde for an hour at room temperature, followed by paraffin-embedding. The paraffin-embedded tissue specimens were cut to produce 5 µm sections. Serial sections were assessed histologically by standard H&E, and RNA ISH. All experiments were performed on matched large and small airway epithelial cells isolated from the same donor lungs and cultured under identical conditions.

Figure 5

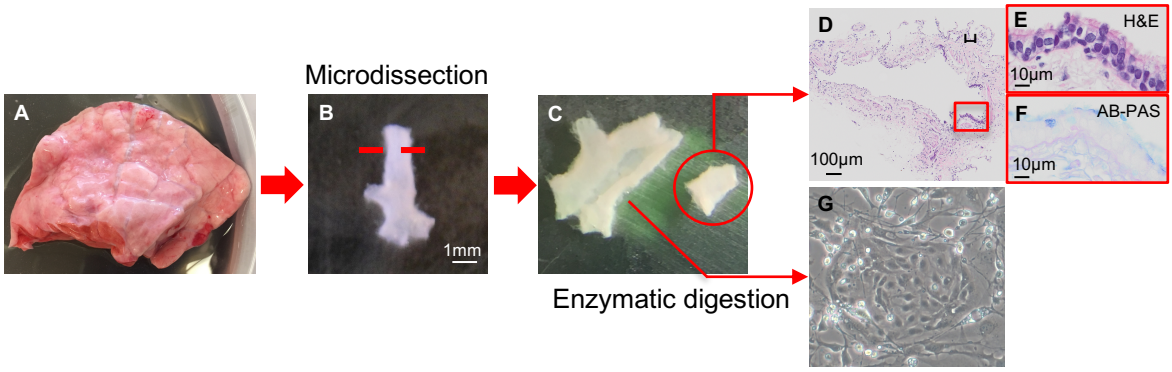

Figure 5. Small airway epithelial cell culture. A-B. A small airway was microdissected from a section of normal human distal lung. C. The dissected small airway was longitudinally cut and small airway epithelial (SAE) cells were isolated by enzymatic digestion. D-F. H&E and AB-PAS staining of the dissected small airway confirmed the presence of airway epithelium and absence of cartilage and submucosal glands within the small airway wall. G. The isolated SAE cells were expanded using a modified conditional reprogramming cell method.

Quantification of MUC5B protein in LAE and SAE cell cultures.

Apical secretions that had accumulated for 7 days were collected from cultured LAE and SAE cells by washing with 200μL PBS, and mucin quantification was carried out using the previously reported protocol (49, 50). Samples were solubilized by addition of urea to reach a 6M urea concentration. Next, samples were reduced with 10 mM dithiothreitol for 90 min at 37 °C and alkylated with 25 mM iodoacetamide for 30 min at room temperature in the dark. Equal volumes of reduced samples (30 μl) were run on 1.2% agarose gel at 80 V for 90 min. Gels were vacuum-blotted onto nitrocellulose membranes with 4X sodium citrate buffer for 2 hours, blocked with Odyssey blocking buffer (OBB, Li-COR Biosciences, Lincoln, NE), and probed with rabbit polyclonal antibodies against MUC5B (H300, 1:2000 in OBB). The secondary antibody was IRDye 680LT donkey anti-rabbit IgG (Li-COR Biosciences), diluted

1:10,000 in OBB. Detection and densitometry were performed using the Odyssey Infrared Imaging System (LI-COR Biosciences). Representative data of technical triplicate were shown for each biological replicate.

RNA extraction and cDNA synthesis.

For RNA extraction from cultured cells and freshly isolated human airway epithelium, TRI Reagent (Sigma) was used according to the manufacturer's instructions. RNA concentrations were determined using a NanoDrop-8000 spectrophotometer (Thermo Scientific, MA, USA). Total RNA was reversed transcribed into cDNA with iScript™ cDNA Synthesis kit (Bio-Rad, CA, USA) according to the manufacturer's instructions. All samples were reverse transcribed under the same conditions. The synthesized cDNA was used in quantitative PCR (qPCR) and ddPCR reactions as a template.

Quantitative PCR TaqMan assays.

qPCR reactions were performed using the Applied Biosystems® 7500 Real-Time PCR Systems (Applied Biosystems, Darmstadt, Germany). Briefly, duplicate reactions were performed using 4 µl first-strand cDNA template, 0.5 µl deionized water, 0.5 µl TaqMan probes and 5 µl SsoAdvanced™ Universal Probes Supermix (Bio-Rad, CA, USA). The thermal cycling conditions were 3 min at 95 °C followed by 40 cycles of 15 sec at 95 °C and 1 min at 60 °C.

For specific gene amplification, the following Taqman Probes (Thermo Fisher Scientific) were used to assess the mRNA levels of following genes: *Glyceraldehyde-3-phosphate dehydrogenase* (*GAPDH*): Hs02758991_g1, *surfactant protein B* (*SFTPB*): Hs00167036_m1. *GAPDH* was used as the reference gene. The quantification of *GAPDH* did not vary between LAE and SAE cells. The PCR products obtained after performing PCR reaction to amplify *SFTPB* and *GAPDH* genes were mixed with ethidium bromide and run on 2% agarose gel at 150 V for 20 min to visualize the amplified cDNA under ultraviolet light.

Absolute quantification of *MUC5AC* and *MUC5B* transcript copy numbers by droplet digital PCR.

Quantitative polymerase chain reaction assays were performed using duplexed FAM and HEX TaqMan assays for *MUC5AC*, *MUC5B*, and *GAPDH*, respectively, in a ddPCR system (QX100; Bio-Rad Laboratories, Inc, Hercules, CA) (51-53). Duplicate TaqMan PCR reaction mixtures of 20 µl were prepared using 2 µl total cDNA, 10 µl ddPCR Supermix for Probes (BioRad), 6 µl RNase/DNase free water, and 1 µl of each 20 × TaqMan Gene Expression Assay (Applied Biosystems, Carlsbad, CA). *GAPDH* assays were performed for each sample on each plate for normalization for all other targets. PCR reactions were dispersed into droplets using the QX100 droplet generator per the manufacturer's instruction (Bio-Rad) and transferred to a 96-well PCR plate. End point PCR was performed in SimpliAmp (Thermo

Fisher Scientific) with the following conditions: 95 °C, 10 min, 94 °C, 30 sec, 60 °C, 1 min, 39 cycles of 94 °C, 30 sec, followed by 60 °C, 1 min, 98 °C, 10 min and cooling to 12 °C. The fluorescence of each droplet was quantified in the QX100 droplet reader (Bio-Rad). Analysis of ddPCR data was performed with QuantaSoft analysis software (Bio-Rad) that accompanied the droplet reader. Thresholds were manually set to distinguish between positive and negative droplets. The output from QuantaSoft included concentration and droplet counts for each target in each well. The concentration for each target gene was normalized to *GAPDH*, and final expression results were reported as target/*GAPDH* ratios. The average target/*GAPDH* ratios for duplicate wells were used. The following Primer/probe mix (Bio-Rad) was used to assess mRNA levels of following genes: *GAPDH*: dHsaCPE5031597; *MUC5AC*: dHsaCPE5055968; *MUC5B*: dHsaCPE5192793.

Mass spectrometry of secretory proteins in LAE and SAE cell culture.

A 100 µl aliquot of apical washes from either LAE or SAE cell culture was diluted 1:1 with GuHCl 8 M, reduced (DTT 10 mM for one hour at 65 °C), alkylated (iodoacetamide 20 mM for 1 hour, room temperature in the dark), and digested with trypsin overnight. Glycopeptides were removed by centrifugation on a 10 kDa filter (Amicon® Ultra Centrifugal filters), samples were freeze-dried and resuspend in formic acid 0.1%. The resulting peptides were analyzed by liquid chromatography-tandem mass spectrometry (Q Exactive, Thermo

Fisher Scientific) as previously described (54). SFTPB was identified and quantified by label-free mass spectrometry, by searching against the most current human database and quantified with Scaffold 4.4.8 (Proteome Software Inc.), using the normalized total precursor intensity, including unique peptides with a minimum of 95% probability by the Scaffold Local FDR algorithm (54). Both MUC5AC and MUC5B were quantified by parallel-reaction monitoring as previously described (55).

RNA ISH in cell pellets made of gene-edited A549 cells.

A549 cells that are deficient in MUC5AC or MUC5B were developed as previously reported (56, 57). A549 cells obtained from the American Type Culture Collection were grown in RPMI 1640, supplemented with 10% fetal bovine serum, penicillin (100 U/ml), streptomycin (100 μg/ml), and glutamine (2 mM) and maintained at 37 °C in a humidified 5% CO_2 atmosphere. We used the lentiviral expressing CRISPR-Cas9 vector generated by the Zhang lab, plentiCRISPRv1.4 for *MUC5B*. This vector system expresses the gRNA, Cas9 protein, and puromycin resistance gene from the virus. The *MUC5B* gRNA was designed using the Zhang lab software available at http://crispr.mit.edu. The gRNA sequence used was 5′-CACCGACCAGCGTCCGGCACGCGCT-3', 5'-CACCGGTGGAACAAAGCTCACGCGC-3', 5'-CACCGTTCAACGTCCAGCTACGCCG-3′, according to Zhang lab protocols (http://www.genome-engineering.org/crispr/?page_id). *MUC5AC* gRNA lentiviral

expressing CRISPR-Cas9 vector was purchased from the Applied Biological Materials Inc. Richmond, BC. The gRNA sequence used was 5'-GTTAAAATCCTCGTAGG-3', 5'-GACCCTGCTCAGCGTGG-3', 5'-GACTTCCGGACCCTCAG-3'. A549 cells were infected with either *MUC5AC* or *MUC5B* CRISPR-Cas9 lentiviral media (viral media diluted in RPMI media, 2 μg/ml polybrene) for 1 hour. At 24 hours post-infection, puromycin (1 μg/ml final concentration) was added to the culture media. Once the gene-edited A549 cells were selected with puromycin, single cells were expanded. At 70-90% confluence, gene-edited A549 cells were collected using 0.25% trypsin. After neutralization of trypsin with 10% fetal bovine serum, gene-edited A549 cells were harvested by centrifugation (2000 rpm, 5 min, 4 °C). Thirty million cells per either MUC5B/MUC5AC, MUC5B or MUC5AC expressing A549 cells were fixed in 50 ml of 10% neutral buffered formalin at room temperature for 24 hours to make cell pellets, and 5 million cells were suspended in 1 ml of TRI Reagent (Sigma) for RNA analysis by ddPCR. After 24 hours of fixation with 10% neutral buffered formalin, the cells were centrifuged and the cell pellets were mixed with agarose, followed by paraffin-embedded. RNA ISH targeting *MUC5B* or *MUC5AC* mRNAs was performed on paraffin-embedded cell pellet sections cut at 5 μm using an RNAscope 2.5 HD Reagent Kit as described above (see RNA *in situ* hybridization in the supplemental methods). The cell pellet sections were scanned and digitized at a magnification 60X using Olympus VS120 light microscope. For quantification of *MUC5B* or *MUC5AC* mRNA-stained areas, the randomly selected fields were captured at

an area of 0.6 mm^2 (= 5000 X 5000 $pixels^2$). The fields captured for quantification in serial sections stained for *MUC5AC*, *MUC5B* mRNAs or positive control was adjusted to be the same location in each section. *MUC5AC* and *MUC5B* mRNA-stained areas were quantified using the same method which was applied to human airway tissues as described above (see Quantification of MUC5AC, MUC5B, and CCSP in AB-PAS, immunohistochemistry and RNA ISH in the supplemental methods). Quantitated *MUC5B* or *MUC5AC* mRNA-stained areas were normalized to the area stained for positive control *UBC* in serial sections and shown as ratios of target/positive control-stained area. Ratios of target/positive control-stained area were compared with absolute quantification of *MUC5AC* and *MUC5B* transcript copy numbers by ddPCR.

Statistical analysis.

Statistics were performed using the R, version 3.5.1 (R Foundation for Statistical Computing). Comparison between two groups was performed by Wilcoxon rank-sum test and comparison between three or more groups was performed by Kruskal-Wallis test, followed by pairwise Wilcoxon rank-sum test for post hoc analysis. A p-value of < 0.05 was considered significant.

5. Results

The regional distribution of mucous glycoproteins in superficial airway epithelium.

AB-PAS staining to quantitate airway regional variations in superficial epithelial mucous glycoproteins, which include MUC5AC and MUC5B, was performed in 10 lungs. Airway GMH, defined as an AB-PAS-stained volume density greater than 0.005 mm^3/mm^2 per airway superficial epithelial region (58), was identified in one or more airway regions in 5 of the 10 subjects (Figure 6A, B). AB-PAS-stained volume densities in subjects with airway GMH were generally greater than those in subjects with histologically normal airways, particularly in larger proximal airways (Figure 6B). Based on the exclusion criteria, the 5 subjects without GMH in any airway region were selected for the RNA ISH and immunohistochemistry study of mucin expression as representative of normal lungs.

Since it is possible that degranulation of the stored mucin protein from superficial epithelial cells occurred during the tissue isolation, which might result in underestimation of AB-PAS- and mucin protein-stained volumes compared to those *in vivo*, we tested whether expression of forkhead box A3 (FOXA3), a transcription factor typically expressed in goblet cells (59), might be helpful in addressing this question. Immunohistochemistry experiments revealed positive signals for FOXA3 protein in the nuclei of goblet cells in airway epithelium with GMH whereas FOXA3 staining was absent in histologically normal airway epithelium (Figure 7). These data suggest that the histologically normal airway epithelium with less AB-

PAS-stained area did not contain the degranulated goblet cells.

Figure 6

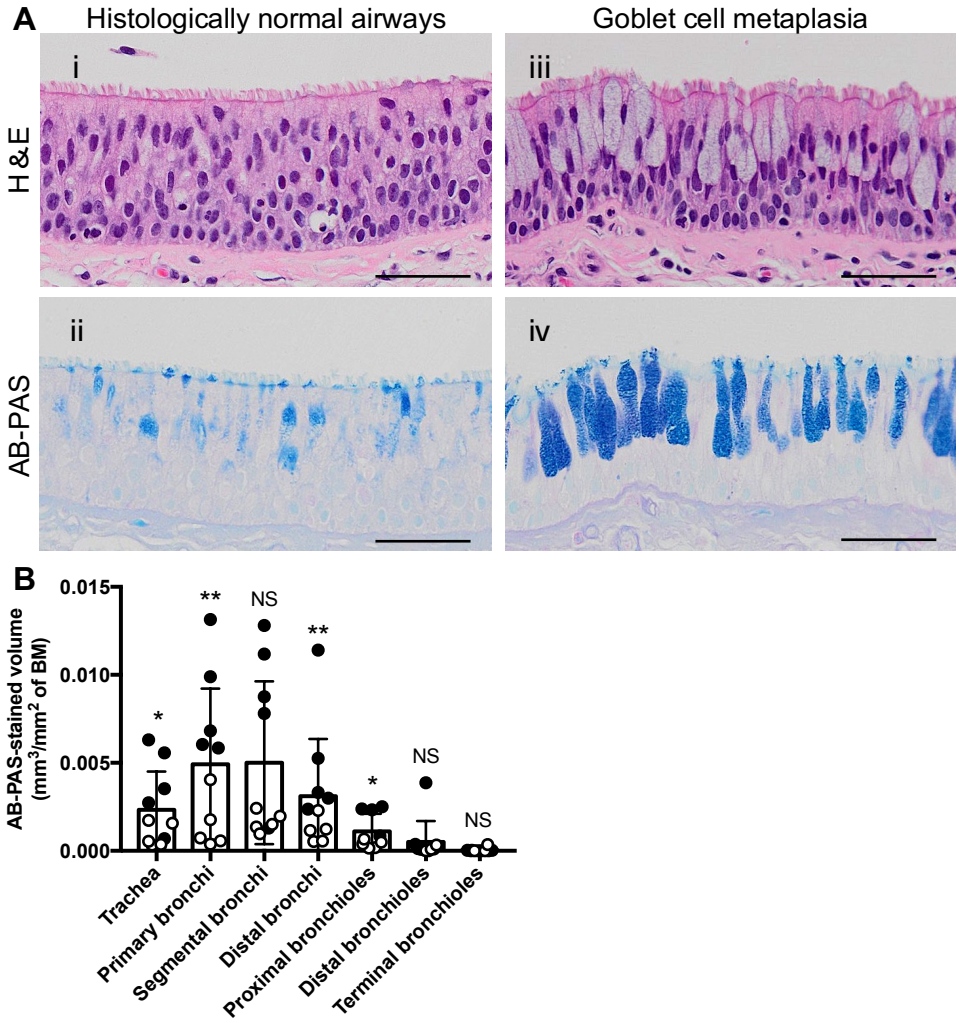

Figure 6. Regional distribution of mucus glycoproteins in superficial airway epithelia from 10 subjects with no prior lung disease history. A. Hematoxylin and eosin (H&E) and alcian blue and periodic acid-Schiff (AB-PAS) staining of the superficial epithelium of primary bronchi in (i, ii) a subject with histologically normal airways versus (iii, iv) a subject with airway goblet cell metaplasia. B. Quantification of AB-PAS-positive mucus glycoproteins in airway superficial epithelium of different airway regions. AB-PAS-stained volume densities in airway superficial epithelium were quantified (n = 10). Each circle represents AB-PAS-stained volume density for each airway region obtained from subjects with histologically normal airways (open circles; n = 5, see Figure 6Ai, ii) and subjects with airway goblet cell metaplasia and/or hyperplasia (GMH) (solid circles; n = 5, see Figure 6Aiii, iv). Mean AB-PAS-stained volume densities in subjects with histologically normal airways were compared with those in subjects with airway GMH by Wilcoxon rank-sum test. Each circle in distal bronchi and bronchioles represent mean values of the AB-PAS-stained volume densities from multiple airways per subject. No proximal bronchiole was available in one of the five subjects with airway GMH. Histobars and error bars depict mean ± SD from the 10 subjects. *: $p < 0.05$, **: $p < 0.01$. BM: basement membrane, NS: not significant. Scale bars = 50 μm.

Figure 7

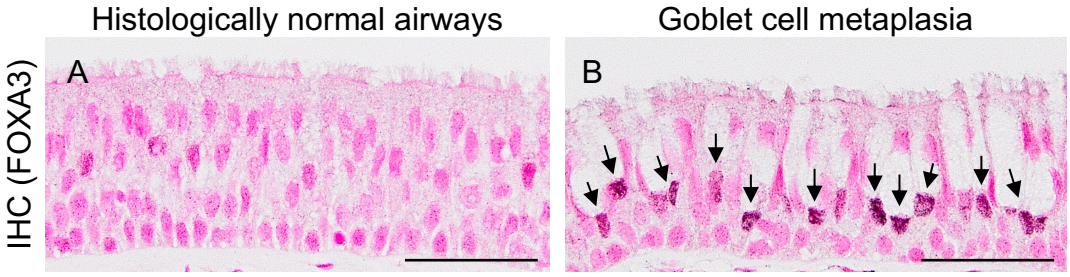

Figure 7. FOXA3 protein localization in a superficial epithelial region of primary bronchi in a subject with histologically normal airways and a subject with airway goblet cell metaplasia. A-B. FOXA3 protein localization stained by immunohistochemistry in primary bronchial superficial epithelium from (A) a subject with histologically normal airways versus (B) a subject with airway goblet cell metaplasia. FOXA3 protein is detected in the nuclei of airway superficial goblet cells (black arrows in panel B) in the subject with airway goblet cell metaplasia whereas FOXA3 staining was absent in histologically normal airway superficial epithelia. Data are representative of three subjects from either subjects with histologically normal airways or subjects with airway goblet cell metaplasia and/or hyperplasia. IHC: immunohistochemistry. Scale bars = 50 μm.

The regional distribution of MUC5B and MUC5AC in histologically normal human airways.

RNA ISH and immunohistochemistry revealed extensive MUC5B, but not MUC5AC, mRNA and protein localization in SMG (Figure 8). Both RNA ISH and immunohistochemistry demonstrated significantly greater stained volume densities for MUC5B, as well as MUC5AC, in the superficial epithelium of larger cartilaginous airways, including the trachea and bronchi, compared to bronchioles (Figure 8-10). Notably, robust MUC5B, but not MUC5AC, mRNA and protein staining were detected in the distal bronchioles. In the terminal bronchioles, neither MUC5B nor MUC5AC was detected.

Figure 8

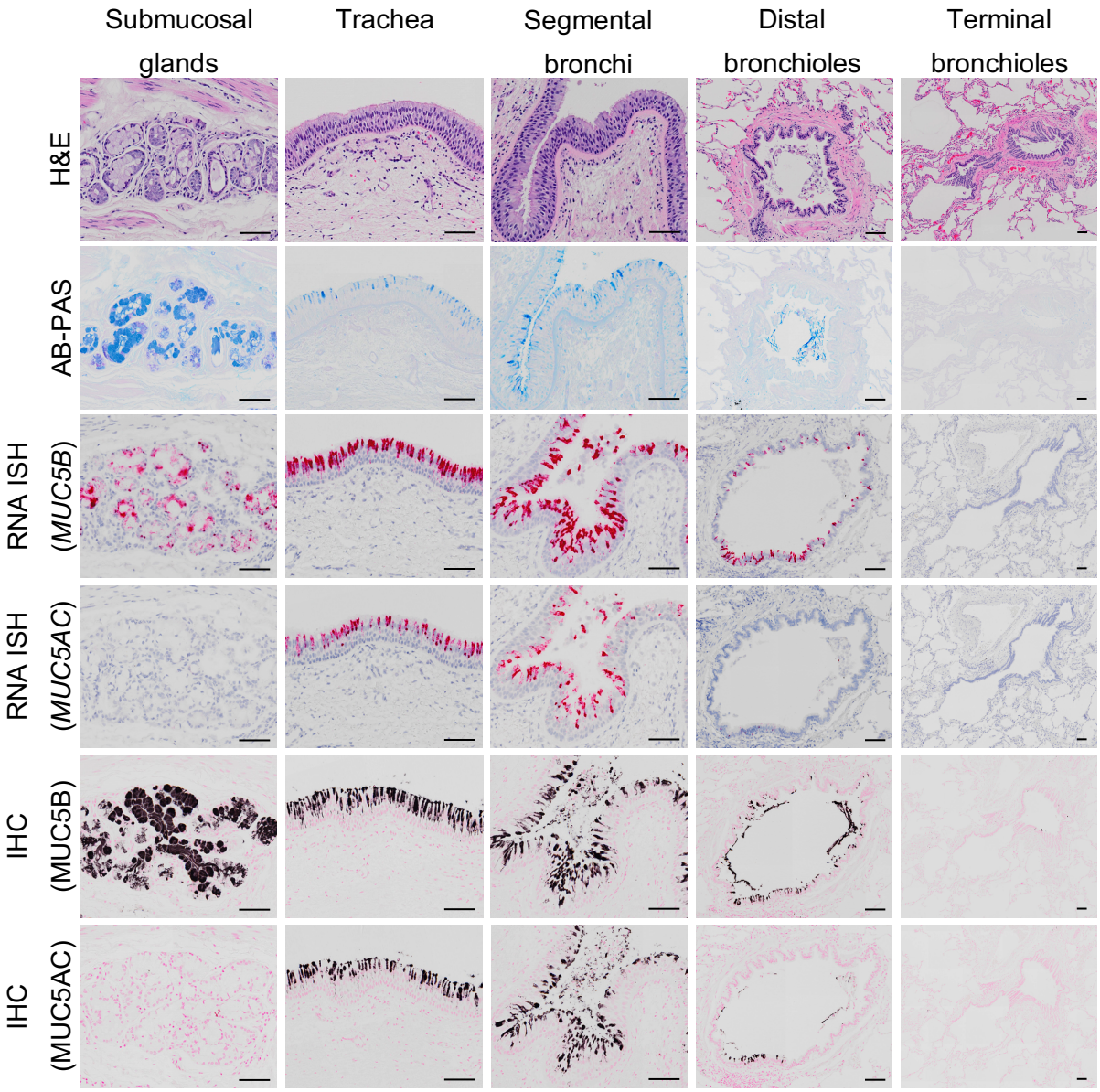

Figure 8. Regional distribution of MUC5B and MUC5AC mRNA and protein localization in histologically normal human airways. Serial sections from five different regions of airways from one histologically normal lung were stained by H&E and AB-PAS, as well as probed for MUC5B and MUC5AC by RNA ISH and immunohistochemistry (IHC). Scale bars = 40 μm. The figure represents a collage of images from this one lung.

Figure 9

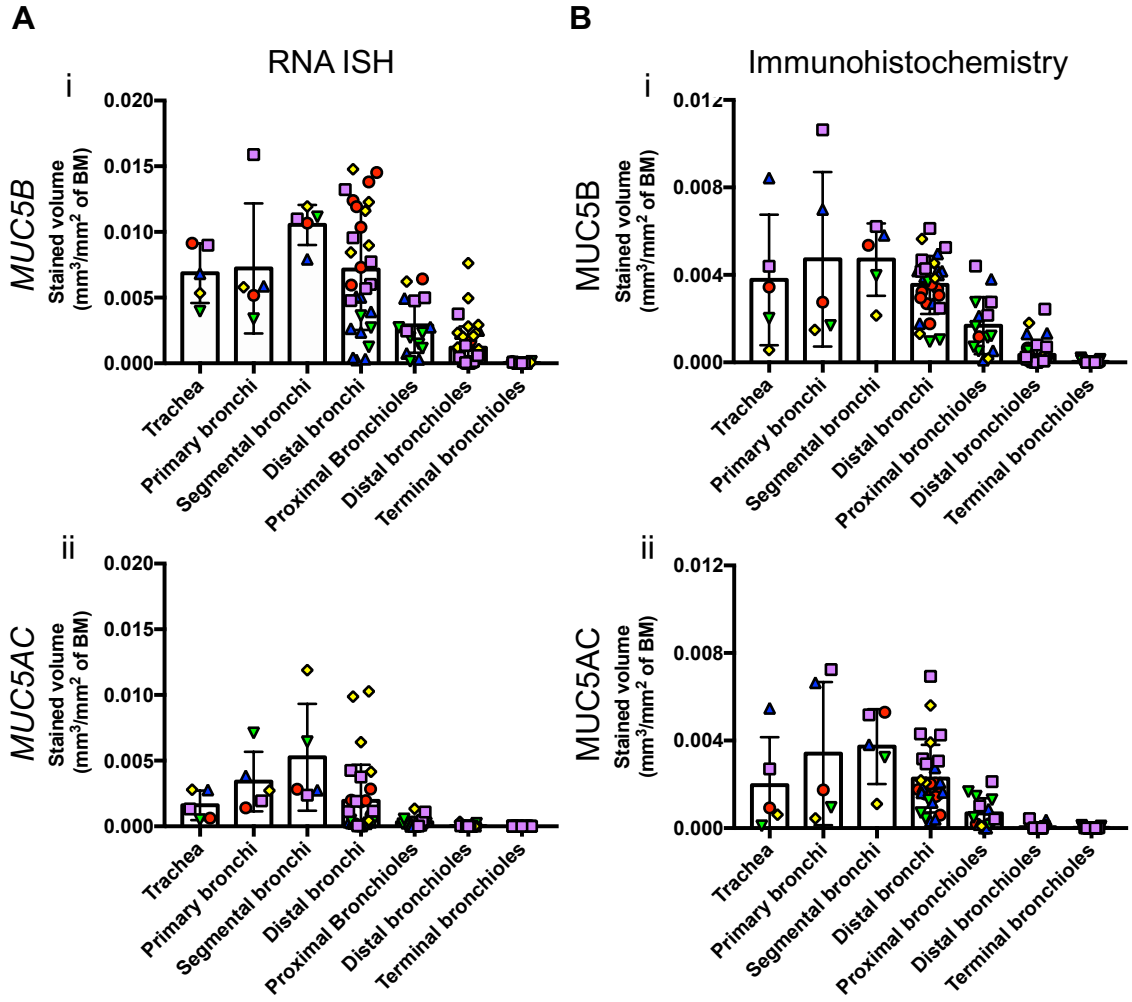

Figure 9. Quantification of MUC5B and MUC5AC mRNAs and proteins in histologically normal human airway superficial epithelia. A. *MUC5B* (Ai) and *MUC5AC* (Aii) mRNA-stained volume densities in airway superficial epithelium from histologically normal lungs were quantified (n = 5). B. MUC5B (Bi) and MUC5AC (Bii) protein-stained volume densities by immunohistochemistry were also quantified (n = 5). Histobars and error bars represent mean ± SD. Symbols represent the five distinct subjects. For distal bronchi and bronchioles, more than one airway per region was examined per subject. BM: basement membrane.

Figure 10

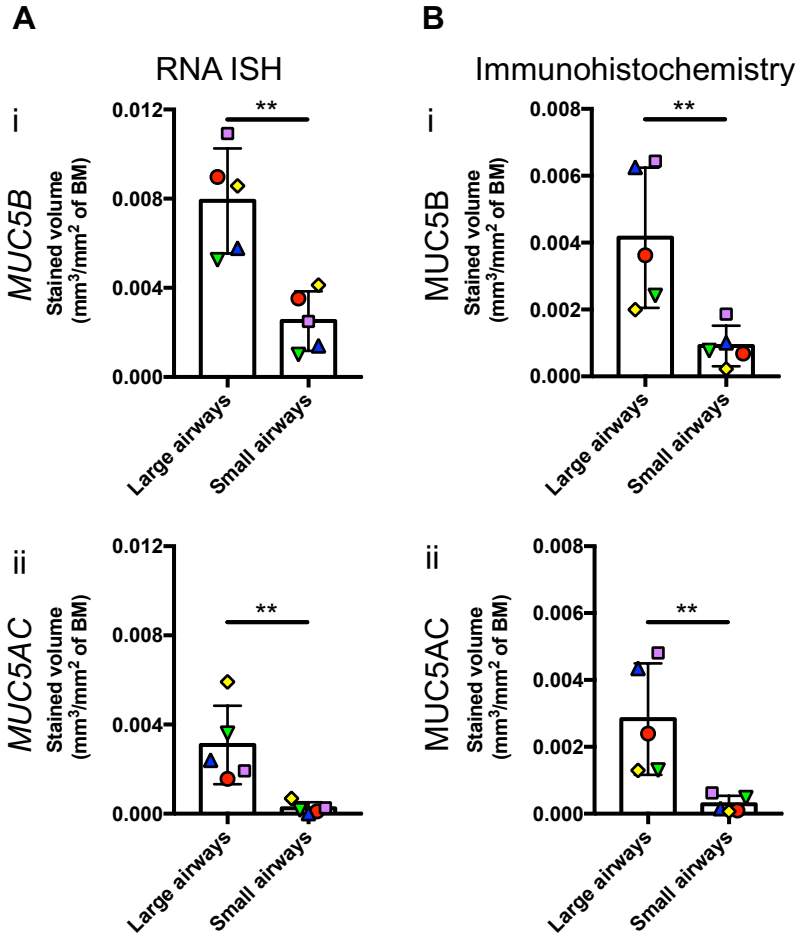

Figure 10. Comparison of MUC5B and MUC5AC mRNAs and proteins between large versus small airway superficial epithelia. A. *MUC5B* (Ai) and *MUC5AC* (Aii) mRNA-stained volume densities within airway superficial epithelium in histologically normal lungs (n = 5) were quantified. B: MUC5B (Bi) and MUC5AC (Bii) protein-stained volume densities by immunohistochemistry were also quantified (n = 5). Symbols in large airways represent mean values of the volume densities of trachea, primary, segmental and distal bronchi, and symbols in small airways represent mean values of the volume densities of proximal and distal bronchioles from the five distinct subjects. These 5 subjects were same as shown in Figure 9. Histobars and error bars represent mean ± SD. BM: basement membrane. *: $p < 0.05$ by Wilcoxon rank-sum test.

Two approaches were utilized to verify the RNA ISH and immunohistochemistry data suggesting that MUC5B is the dominant mucin in bronchioles. First, the relative sensitivities of the RNA ISH *MUC5B* versus *MUC5AC* probes were tested by comparing RNA ISH versus ddPCR signals in pellets derived from clustered regularly interspaced short palindromic repeats (CRISPR)/CRISPR-associated protein 9 (Cas9)-modified A549 cells expressing *MUC5AC* and *MUC5B*, *MUC5AC* only, or *MUC5B* only. Data from three independent experiments revealed that the *MUC5B* probe exhibited 2.1 ± 0.3-fold increased sensitivity compared to *MUC5AC* (Figure 11). Adjusting the RNA ISH data by this factor did not alter the conclusion that *MUC5B* was the dominantly expressed mucin in bronchioles.

Figure 11

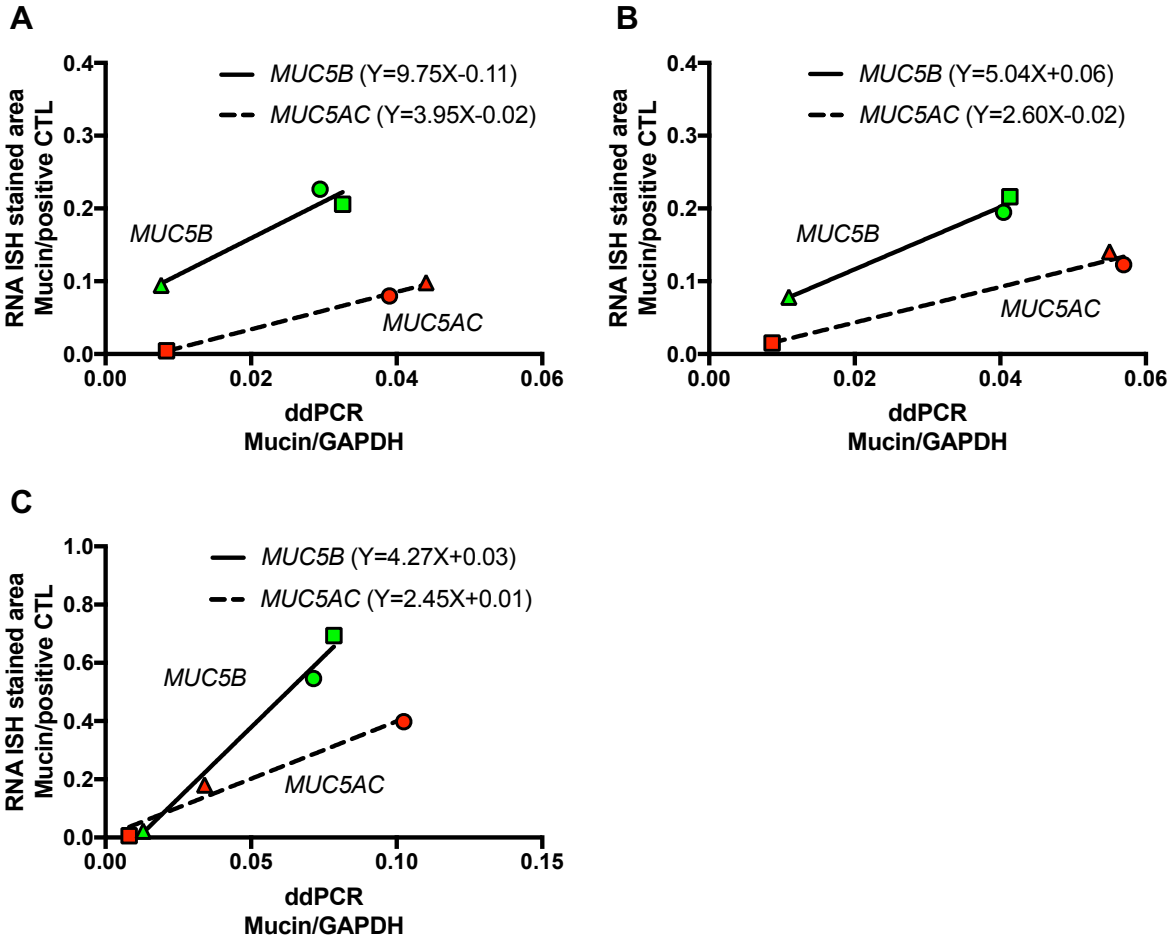

Figure 11. Differential affinity of RNA ISH probes for *MUC5B* and *MUC5AC* mRNAs. The relative sensitivities of the RNA ISH *MUC5B* versus *MUC5AC* probes were tested by comparing RNA ISH stained area versus ddPCR signals for *MUC5B* and *MUC5AC* mRNAs in cell pellets derived from genetically modified A549 cells expressing *MUC5AC*/*MUC5B* (circles), *MUC5B* (squares), or *MUC5AC* (triangles) mRNAs. A-C. Three independent experiments were performed. Quantitated *MUC5B* or *MUC5AC* mRNA-stained areas in the randomly selected fields were normalized to the area stained for positive control *UBC* in serial sections and shown as ratios of target to positive control-stained area. Quantitated absolute *MUC5B* or *MUC5AC* transcript copy numbers by ddPCR were normalized to *GAPDH* and shown as target/*GAPDH* ratios. R^2 was high for each group, ranging from 0.9336 to 0.9971. RNA ISH: RNA *in situ* hybridization, CTL: control, ddPCR: droplet digital PCR.

Second, sections from large versus small airways were obtained from 6 normal lungs, and ddPCR of superficial epithelia from each region was performed to compare *MUC5B* to *MUC5AC* transcript copy number in each airway region (Figure 12). Absolute quantification of *MUC5B* and *MUC5AC* transcripts revealed that *MUC5B* normalized to *GAPDH* (*MUC5B*/*GAPDH*) was not different from *MUC5AC*/*GAPDH* in the larger cartilaginous airways, including trachea and bronchi. In contrast, *MUC5B*/*GAPDH* was significantly greater than *MUC5AC*/*GAPDH* in bronchioles (Figure 12B). Based on the *MUC5AC*/*MUC5B* ratio (Figure 12C), *MUC5B* transcript copy number was 20-fold higher than *MUC5AC* in bronchioles, consistent with RNA ISH/immunohistochemistry data.

Figure 12

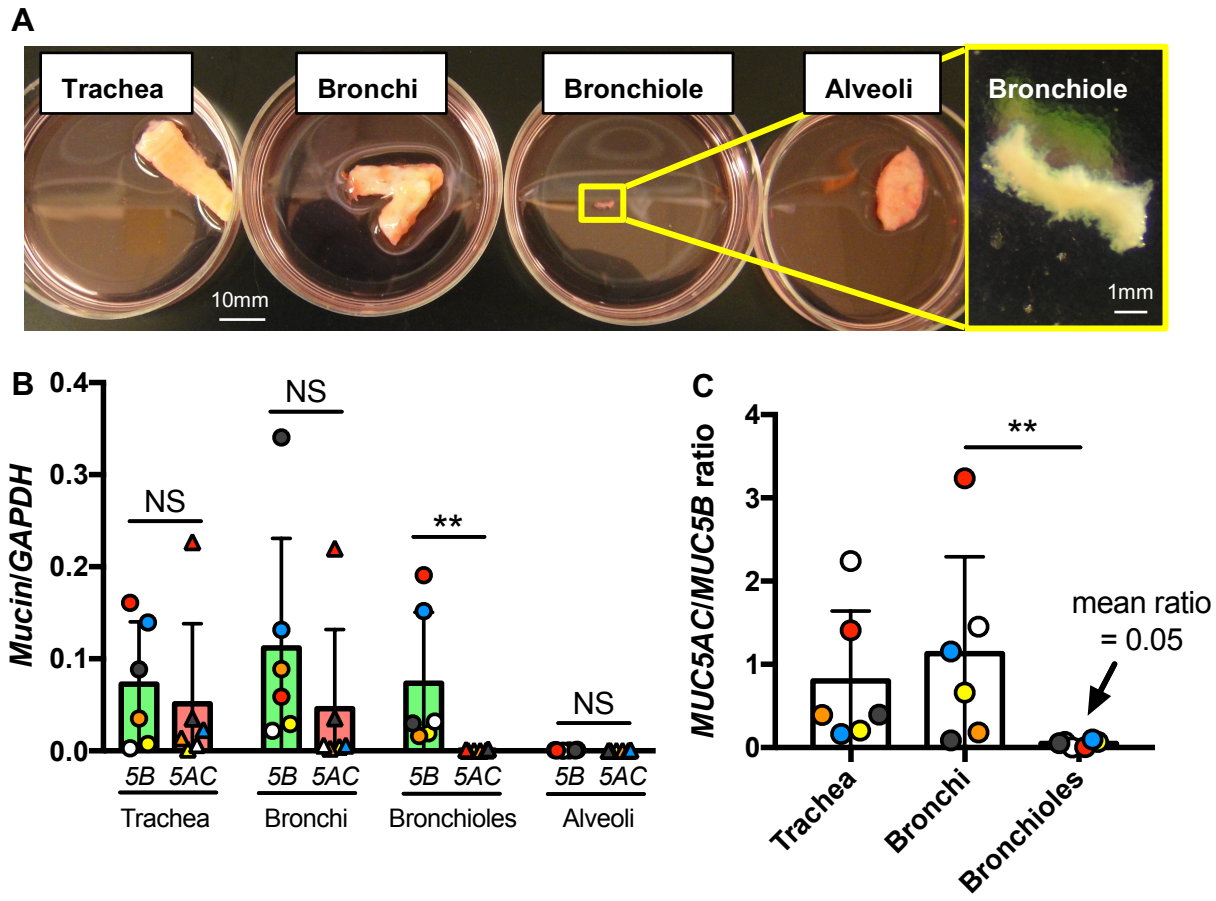

Figure 12. Droplet digital PCR quantification of *MUC5B* and *MUC5AC* transcript copy numbers in freshly isolated human airway epithelium from subjects with no prior lung disease history. A. Examples of dissected airway tissues including a trachea, bronchi, bronchiole and peripheral lung parenchyma. B. Absolute transcript copy numbers in different airway regions for *MUC5B* (circles) and *MUC5AC* (triangles). C. *MUC5AC*/*MUC5B* ratios in each airway region. Measurements in panels B and C were performed by droplet digital PCR, with absolute *MUC5B* or *MUC5AC* transcript copy numbers normalized to *GAPDH* and shown as target/*GAPDH* ratios. Histobars and error bars represent mean ± SD. n = 6. Different symbol colors indicate results from 6 distinct individual subjects. **: $p < 0.01$ by Wilcoxon rank-sum test. NS: not significant.

What cell type expresses *MUC5B* and *MUC5AC* mRNAs in histologically normal human large and small airways?

Based on mouse airway data (17-21), CCSP+ secretory cells were identified as candidates for secretory mucin expression in normal human airways. Both RNA ISH and immunohistochemistry demonstrated widespread superficial epithelial localization of CCSP mRNA and protein from the trachea to the terminal bronchioles (Figure 13A-D, 14). With respect to SMG, *CCSP* mRNAs were expressed in the ciliated ducts but not collecting ducts nor acini (Figure 13E, F). In contrast, *MUC5B* mRNAs were localized throughout all SMG epithelial structures. Quantification of *CCSP* mRNA-stained volume densities revealed robust expression in the segmental, distal bronchi and bronchioles compared to trachea or primary bronchi (Figure 13G).

Figure 13

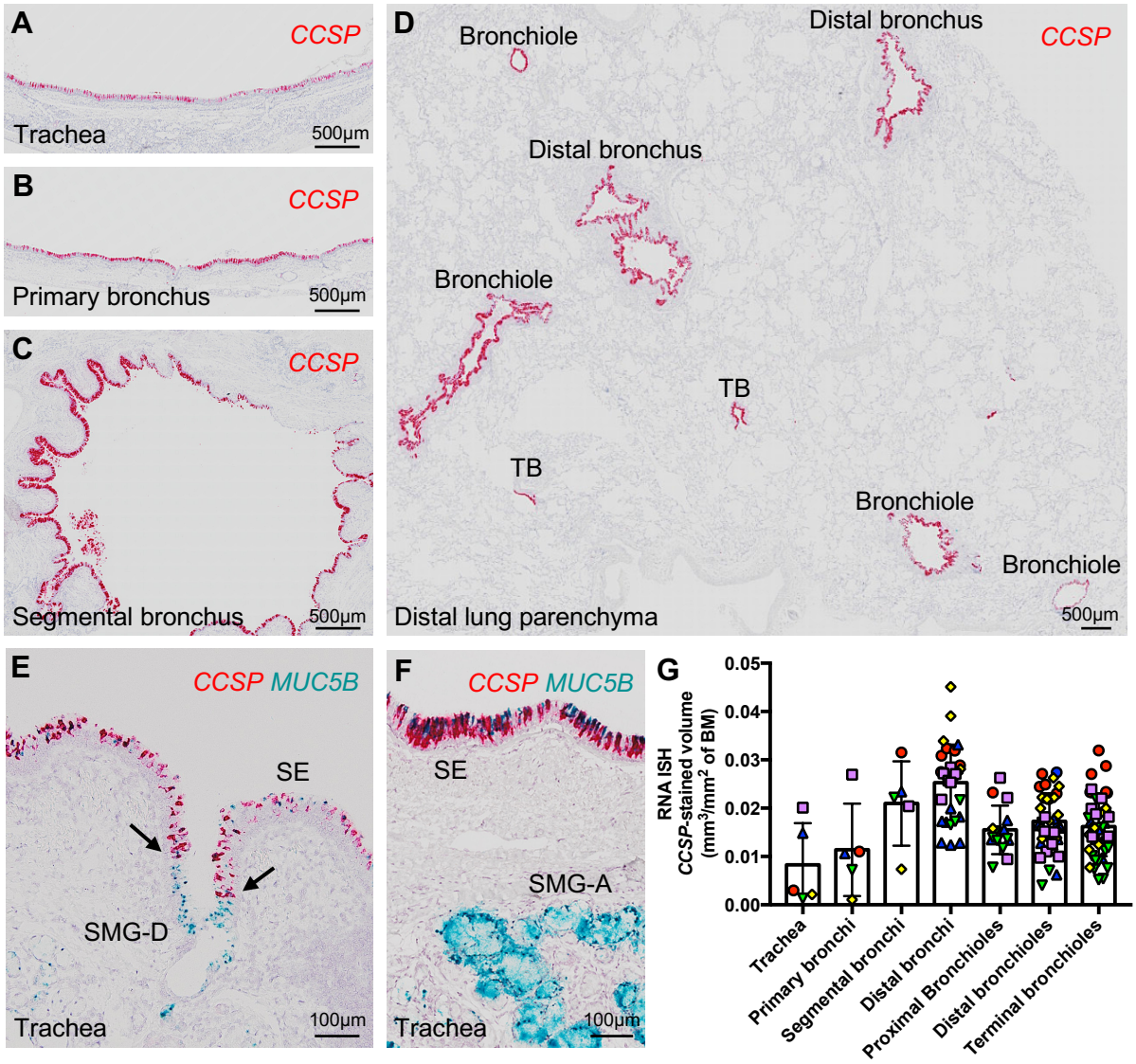

Figure 13. Regional distribution of *CCSP* mRNA localization in histologically normal human airways. A-D. Representative *CCSP* mRNA localization from one histologically normal lung stained by RNA ISH in (A) trachea, (B) primary bronchus, (C) segmental bronchus and (D) distal lung parenchyma containing distal bronchi and bronchioles. E. *CCSP* and *MUC5B* mRNA localization stained by RNA ISH in histologically normal tracheal submucosal gland ducts (SMG-D). *CCSP* (red) mRNA signals stop in the middle of the SMG-D (arrows) with *MUC5B* (teal) mRNA signals being expressed throughout the SMG-D. F. *CCSP* and *MUC5B* mRNA localization co-stained using RNA ISH in the histologically normal tracheal superficial epithelium (SE) and submucosal gland acini (SMG-A). G. Quantification of *CCSP* mRNA-stained volume densities in histologically normal human airway superficial epithelium (n = 5). *CCSP* mRNA-stained volume densities by RNA ISH were quantified. Histobars and error bars represent mean ± SD. Symbols represent the five distinct subjects. For distal bronchi and bronchioles, more than one airway per region was examined per subject. TB: terminal bronchiole, BM: basement membrane.

Figure 14

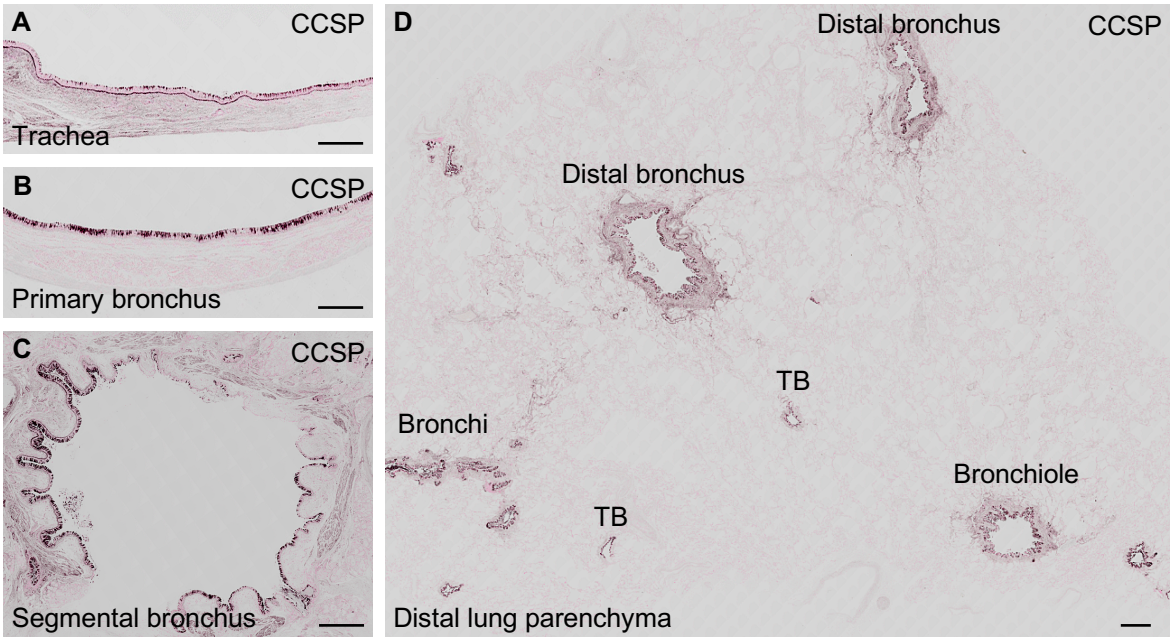

Figure 14. Regional distribution of CCSP protein localization in histologically normal human airways. A-D. Representative CCSP protein localization stained by immunohistochemistry in one histologically normal human lung: (A) trachea, (B) primary bronchus, (C) segmental bronchus, and (D) distal lung parenchyma containing distal bronchi, bronchioles and terminal bronchioles (TB). Scale bars = 500 μm.

Quantitative co-localization studies were performed using fluorescent RNA ISH in 5 histologically normal lungs (Figure 15). Typical goblet cells, characterized by AB-PAS positive large secretory vesicles filling the cytoplasm, were rarely identified in superficial epithelia of these subjects (Figure 15Bii). In contrast, SMG consistently exhibited mucous cells with AB-PAS definable large mucin granules (Figure 15Aii).

Human airway cells expressing *MUC5AC*, *MUC5B*, *CCSP* mRNAs, or a combination of these markers were classified into the 7 possible types (Figure 15). Four distinct, region-specific dominant cell types were identified amongst the 7 possible types. First, *CCSP*-

/*MUC5B*+/*MUC5AC*- cells were routinely found in SMG yet rarely, if at all, in superficial epithelia. Second, *CCSP*+/*MUC5B*+/*MUC5AC*+ cells were the dominant cell type in primary bronchial superficial epithelia. In this region, H&E and AB-PAS staining identified two non-ciliated epithelial cell types: 1) a non-ciliated epithelial cell which had an AB-PAS-stained apical bulge protruding into the airway lumen; and 2) a cell with apical cell membranes at the same height as those of adjacent ciliated cells without an apical bulge (Figure 15Bi, ii). *CCSP*+/*MUC5B*+/*MUC5AC*+ cells exhibited morphologies similar to both cell types (Figure 15Bvii). The number of *CCSP*+/*MUC5B*+/*MUC5AC*+ cells dramatically decreased in the bronchioles, and virtually disappeared in the terminal bronchioles, paralleling the decreased volume densities of *MUC5AC* mRNA and protein (Figure 9). Third, *CCSP*+/*MUC5B*+/*MUC5AC*- cells were the dominant cell type in the distal bronchiolar superficial epithelium. H&E staining identified non-ciliated epithelial cells with dome-shaped apical bulges which morphologically corresponded to the *CCSP*+/*MUC5B*+/*MUC5AC*- cells (Figure 15Ci, vii). Finally, although a small number of *CCSP*+/*MUC5B*+/*MUC5AC*- cells were detected, *CCSP*+/*MUC5B*-/*MUC5AC*- cells were the dominant cell type in the terminal bronchioles. Of note, *CCSP*+/*MUC5B*- cells in superficial epithelia of terminal bronchioles uniquely expressed *SFTPB*, which is known as a distal airway marker (60) (Figure 16).

Figure 15

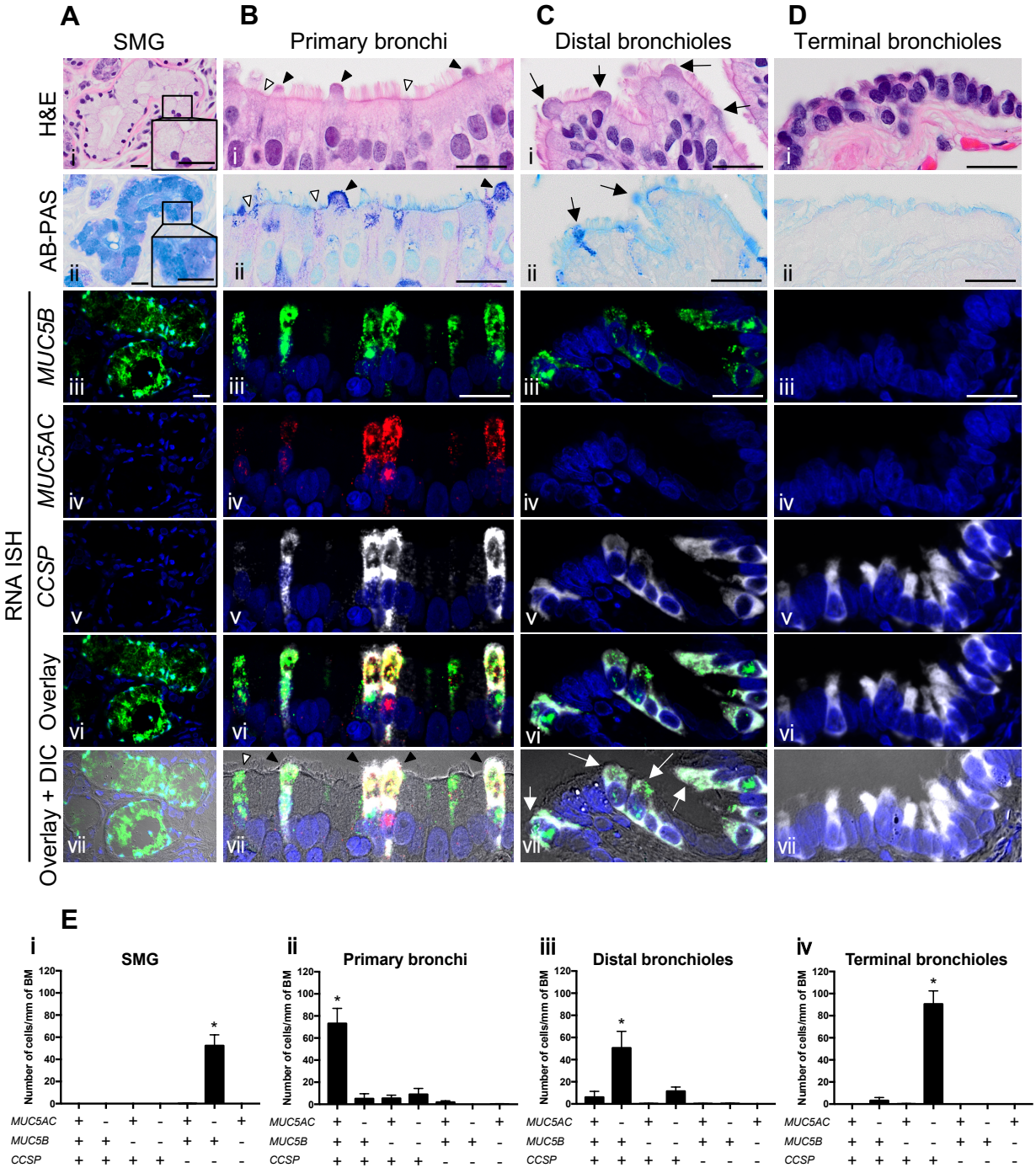

Figure 15. *MUC5B*, *MUC5AC*, and *CCSP* mRNA co-expression is region-specific. A-D. Co-localization of *MUC5B* and *MUC5AC* with *CCSP* mRNAs by RNA ISH in four different regions of histologically normal human airways. For cellular localization, *MUC5B* (green), *MUC5AC* (red), and *CCSP* (white) mRNAs were visualized by fluorescent RNA ISH. Single color images were merged (Avi - Dvi, "overlay") and the overlaid images superimposed on differential interference contrast (DIC) (Avii - Dvii). In submucosal glands (SMG) (A), mucus cells exhibited AB-PAS definable large mucin granules (insets in Ai, Aii). In primary bronchial superficial epithelium (B), two non-ciliated epithelial cell types were identified: 1) a non-ciliated epithelial

cell with an AB-PAS-stained apical bulge (Bi, Bii, and Bvii, black arrowheads); and 2) a non-ciliated epithelial cell without the apical bulge (Bi, Bii, and Bvii, white arrowheads). In distal bronchioles (C), non-ciliated epithelial cells with dome-shaped apical bulges (Ci, Cii, black arrows) corresponded to the *CCSP*+/*MUC5B*+/*MUC5AC*- cells (Cvii, white arrows). Nuclei were stained with DAPI (blue). Scale bars = 20 μm. E. Quantification of cell types expressing *MUC5B*, *MUC5AC* and/or *CCSP* mRNAs in different regions of histologically normal human airways. Data are expressed as the number of each cell type per mm of basement membrane (BM). Solid bars and error bars represent mean ± SD. n=5. *: $p < 0.05$ compared to every other cell type by pairwise Wilcoxon rank-sum test for post hoc analysis, following significant Kruskal-Wallis test.

Figure 16

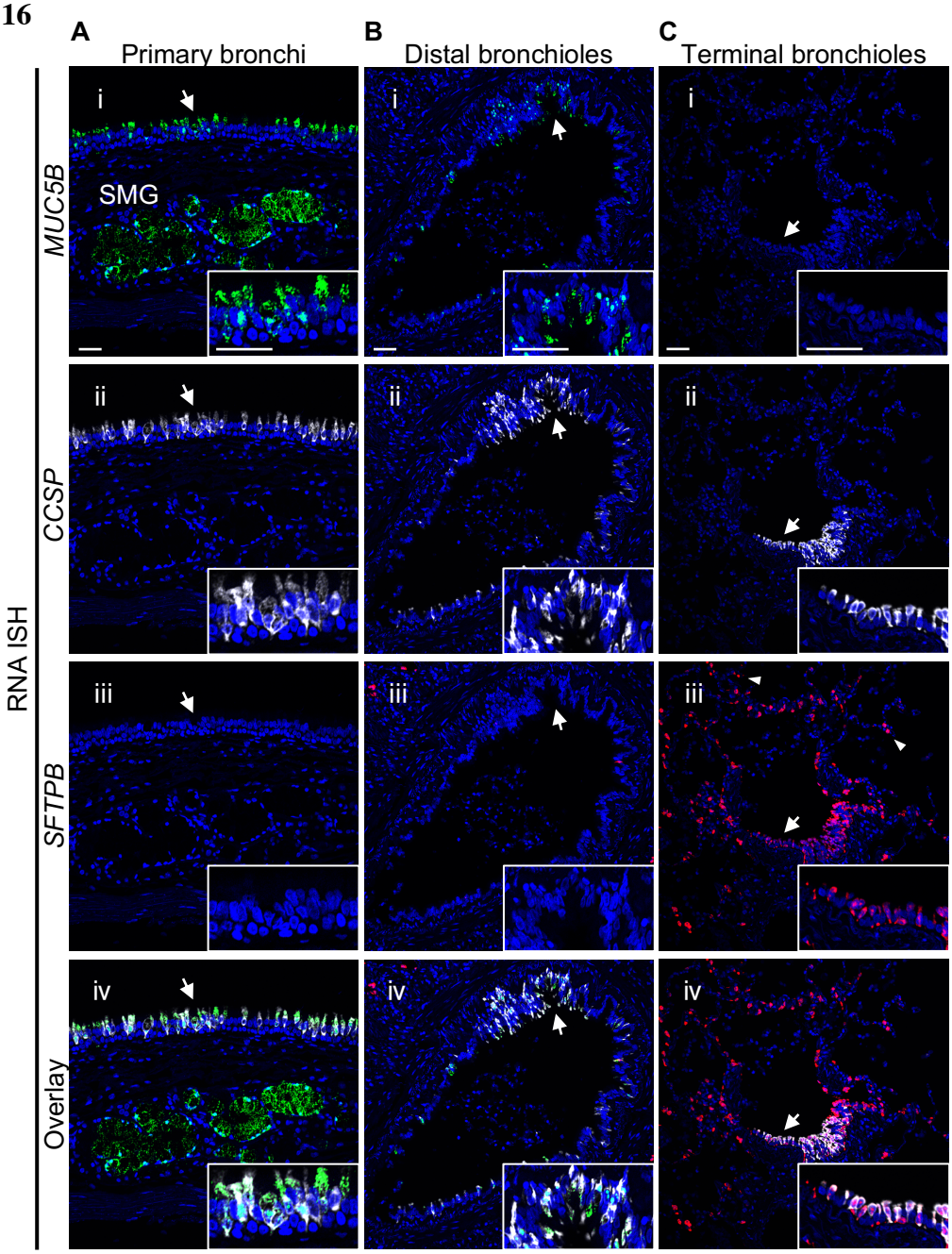

Figure 16. Region-specific localization of *SFTPB* mRNAs in histologically normal human airways. A-C. *MUC5B*, *CCSP*, and *SFTPB* mRNA localization by RNA ISH in three different regions of airways from one representative histologically normal lung. For cellular localization, *MUC5B* (green), *CCSP* (white), and *SFTPB* (red) mRNAs were visualized by fluorescent RNA ISH. Single color images were merged (Avi - Cvi, "overlay"). *SFTPB* mRNAs are uniquely localized in superficial epithelium of terminal bronchioles where *MUC5B* mRNAs are absent (Ci, Ciii). In the terminal bronchiolar superficial epithelium, *SFTPB* mRNAs are co-expressed with *CCSP*+/*MUC5B*- cells (inset in Civ). *SFTPB* mRNAs are also localized in alveolar type II cells (white arrow heads in Ciii). In contrast, *SFTPB* mRNAs are not localized in distal bronchioles where *MUC5B* mRNAs are present (Bi, Biii). Insets show regions indicated by white arrows. Nuclei were stained with DAPI (blue). SMG: submucosal glands. Scale bars = 50 μm.

Primary human small airway epithelial cells secrete MUC5B protein *in vitro*.

Based on the reported distinct progenitor cell properties of large versus distal airway epithelial cells (40, 60, 61), we utilized an SAE versus LAE cell culture technique to test whether MUC5B protein was locally produced by small airway epithelia as predicted by *in vivo* RNA ISH and immunohistochemistry data. H&E staining revealed monolayer epithelia in SAE cell cultures versus stratified multilayers in LAE cells (Figure 17Ai, ii), consistent with *in vivo* morphological features of large versus small airway epithelium in human lungs (62, 63). As a distal airway marker (60), SFTPB was detected by quantitative PCR and mass spectrometry in SAE but not LAE cultured cells (Figure 17B, D). These findings indicate that our *in vitro* SAE cell culture model retained characteristics of distal airways distinguishable from large airways.

RNA ISH showed *MUC5B* mRNA localization in *CCSP* mRNA+ non-ciliated secretory cells in both LAE and SAE cells (Figure 17A iii-vi). Both Western blotting and mass spectrometry identified MUC5B protein in apical washes of SAE cells (Figure 17C, E) though less than secreted by LAE cells. In apical washes obtained from SAE cells, the concentration of MUC5B protein (6.04 ± 5.95 pmol/ml) was 9.2-fold higher than MUC5AC (0.66 ± 0.20 pmol/ml) (Figure 17F).

Figure 17

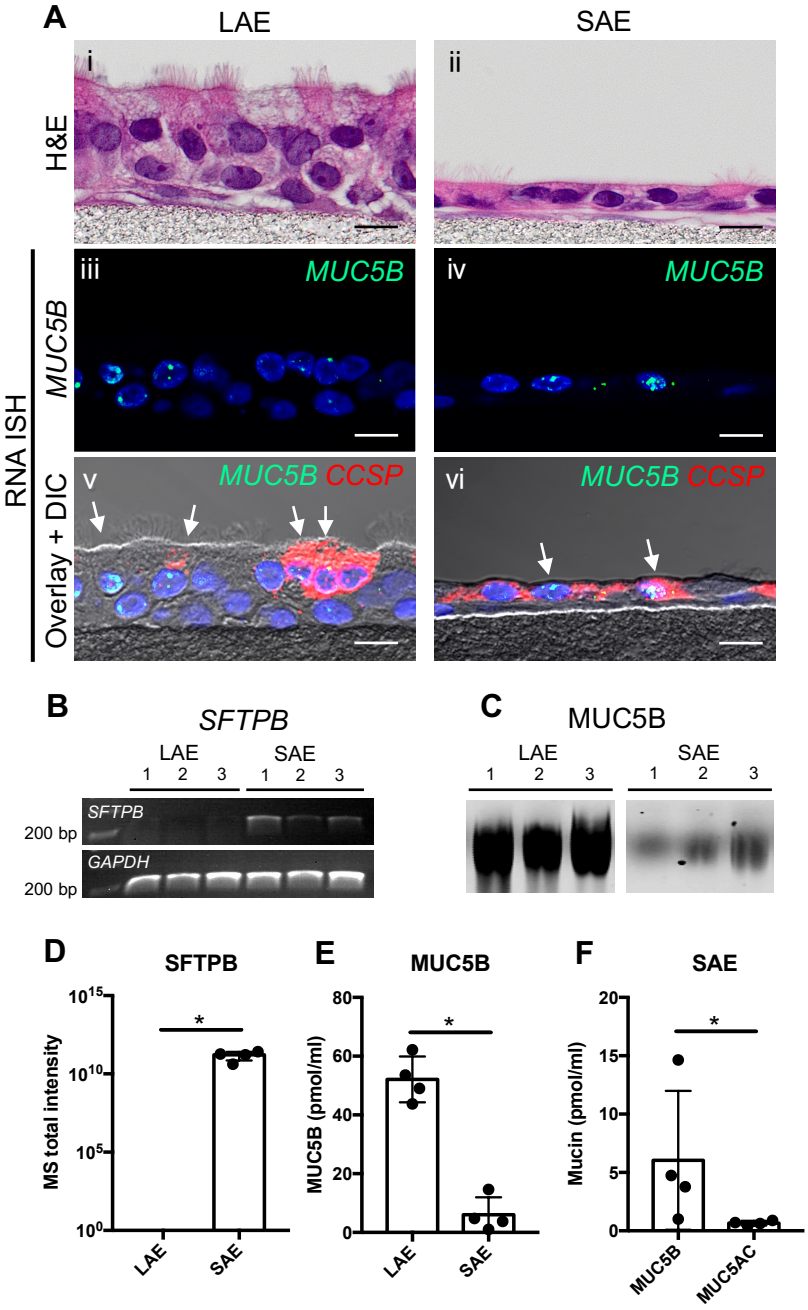

Figure 17. MUC5B production in primary human small airway epithelial cell cultures. A. Histologic images of large and small airway epithelial cell cultures. Air-liquid interface cultures of large airway epithelial (LAE) and small airway epithelial (SAE) cells were stained by H&E (i, ii) and RNA ISH for *MUC5B* (iii, iv) and *CCSP* mRNAs (v, vi). *MUC5B* mRNAs (green) are localized in *CCSP* mRNA (red) positive non-ciliated cells in both LAE and SAE cells (v, vi, white arrows). Scale bars = 10 μm. B. *SFTPB* transcript expression in LAE and SAE cells. *SFTPB* gene was specifically detected in SAE but not LAE cells by quantitative PCR. *GAPDH* was used as the reference gene. C. Identification of MUC5B protein in apical washes of LAE and SAE cells. Immunoblots of apical washes were probed with antibody to MUC5B. Samples from both LAE and SAE cell cultures were run on the same gel. D. Quantification of SFTPB protein in apical washes of LAE and SAE cells. SFTPB protein was identified by mass spectrometry (MS) using

label-free quantification normalized to total precursor intensity. E. Absolute concentrations of MUC5B protein in apical washes of LAE and SAE cells as determined by MS. F. Absolute mucin concentrations for both MUC5B and MUC5AC in apical washes of SAE cells as determined by MS. Panels B and C: n = 3, the order of 3 biological replicates were same in the panel B and C. Panels D-E: Histobars and error bars represent mean ± SD. n = 4, *: $p < 0.05$ by Wilcoxon rank-sum test.

Region-specific superficial epithelial mucin production in histologically normal human lungs.

To describe the airway regions contributing to total MUC5AC and MUC5B expression in the lung, the numbers, diameters, and total surface areas of airways as reported by Weibel *et al*. (46, 47) were utilized to calculate: 1) total *MUC5B*, *MUC5AC* or *CCSP* mRNA-stained volumes for the superficial epithelium of each airway region based on RNA ISH; and 2) the percent of total *MUC5B*, *MUC5AC* and *CCSP* mRNA-stained volumes for each airway region (Figure 18, Table 4).

MUC5B mRNA-stained volume in airway superficial epithelia increased from the proximal to the distal airways, reflecting the exponential increase in distal airway surface area. *MUC5B* mRNA-stained volume peaked in the distal bronchioles with a 3-fold higher value than observed in the cartilaginous large airways. In contrast, *MUC5AC* mRNA-stained volume peaked in the distal bronchi. Even though the combined surface area of proximal and distal bronchioles is > 30-fold greater than distal bronchi, the percent of *MUC5AC* mRNA-stained volumes in bronchioles was less than distal bronchi. Importantly, both *MUC5B* and *MUC5AC* mRNA-stained volumes were negligible in the terminal bronchioles despite the fact that

terminal bronchiolar surface area is the largest of the airway regions. For reference, *CCSP* mRNA-stained volume increased as a function of more distal regions and peaked in the terminal bronchioles.

Figure 18

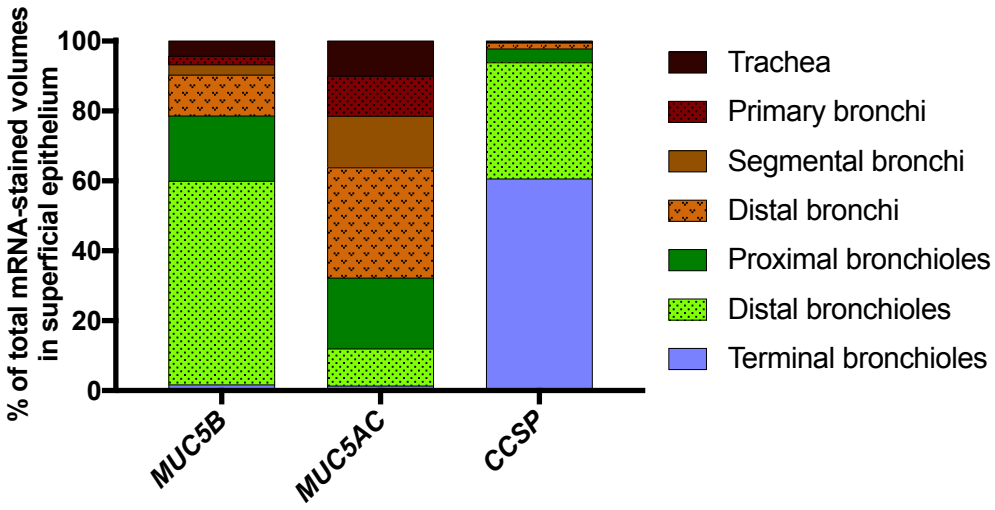

Figure 18. Distinct regional distributions of *MUC5AC*, *MUC5B* and *CCSP* mRNA localization in superficial epithelium of the histologically normal lung. Data represent the calculated percent of total *MUC5AC*, *MUC5B* or *CCSP* mRNA-stained volumes for each airway region. Total *MUC5AC*, *MUC5B* or *CCSP* mRNA-stained volume for each airway region was calculated by multiplying the mean values of the RNA ISH volume densities for each airway region obtained from 5 histologically normal lungs by predicted total surface area of corresponding airway regions.

Table 4: Stained volume densities for *MUC5B*, *MUC5AC*, and *CCSP* mRNAs within superficial airway epithelium

					RNA ISH stained volume densities in SE (mm^3/mm^2 of BM)†		
Classification of airway region	Airway generation*	Airway diameter (cm)*	Number per generation (n)*	Total airway surface area without alveoli (cm^2)*	*MUC5B*	*MUC5AC*	*CCSP*
Trachea	0	1.8	1	67.86	6.86E-03	1.60E-03	8.27E-03
Primary bronchi	1	1.22	2	36.49	7.22E-03	3.41E-03	1.14E-02
Segmental bronchi	2	0.83	4	19.82	1.05E-02	5.26E-03	2.10E-02
	3	0.56	8	10.70			
Distal bronchi	4	0.45	16	28.73	7.14E-03	1.94E-03	2.53E-02
	5	0.25	32	26.89			
	6	0.28	64	50.67			
	7	0.23	128	70.29			
Proximal bronchioles	8	0.186	256	95.74	2.89E-03	3.17E-04	1.55E-02
	9	0.154	512	133.76			
	10	0.130	1024	192.37			
	11	0.109	2048	273.51			
Distal bronchioles	12	0.095	4096	403.41	1.19E-03	2.18E-05	1.73E-02
	13	0.082	8192	569.79			
	14	0.074	16384	876.05			
	15	0.066	32768	1358.86			
	16	0.060	65536	2038.29			
Terminal bronchioles	17	0.054	131072	2759.02	1.76E-05	1.42E-06	1.62E-02
	18	0.050	262144	3613.32			
	19	0.047	524288	3831.98			
Alveolar	20	0.045	1048576	0	N. A.	N. A.	N. A.
	21	0.043	2097152	0			
	22	0.041	4194304	0			
	23	0.041	8388608	0			

*: Values were obtained from references 46 and 47. †: RNA ISH stained volume densities in superficial epithelium (SE) for each airway region were calculated by multiplying the mean values of the RNA ISH volume densities for each airway region obtained from five histologically normal lungs by predicted total surface area of corresponding airway regions. RNA ISH = RNA *in situ* hybridization; BM = basement membrane; N. A. = not applicable.

6. Discussion

A comprehensive regional expression pattern of MUC5B and MUC5AC in normal human lungs has not been reported. Recent data from mice airways suggest that Muc5b is secreted by superficial epithelial club cells in both larger airways and bronchioles (16-19). Whether this paradigm pertains to normal human airways was the focus of this study.

Our results demonstrate that MUC5B is extensively expressed in the superficial epithelium, in addition to SMG, of histologically normal human airways. Importantly, these findings indicate that a major site for MUC5B production is the small airway superficial epithelia where SMG do not exist (Figure 18). These findings are consistent with: 1) the results of RNA-seq quantification of the normal human small airway epithelial transcriptome (64); and 2) studies describing high expression of MUC5B versus MUC5AC in normal distal airway epithelium (25).

Our studies permitted a semi-quantitative description of the relative expression of MUC5B in the SMG versus small airways of the histologically normal human lung. In the large airways, *e.g.,* from trachea to 6th generation bronchi, SMG occupy a volume of ~0.10 mm^3/mm^2 airway surface area in non-smokers (65), and the mucous cell percentage of total SMG volume is about 40% (66, 67). Based on these numbers and regional airway surface areas (46, 47) (Table 5), the *MUC5B* mRNA-stained volume in distal bronchiolar superficial epithelia exceeded the total mucin volume of the SMG (Figure 19). Although it is difficult to predict

secretion rates based on stained volumes, the superficial epithelium of small airways may be considered a source of MUC5B production at least equal to SMG.

Table 5: MUC5B-stained volumes in superficial epithelium versus submucosal glands in larger cartilaginous airways

Classification of airway region	RNA ISH *MUC5B*-stained volumes in SE (μl)	Airway generation*	Volume of glands (mm^3/mm^2)*	Mean volumes of glands per each airway region (mm^3/mm^2)	Total airway surface area (cm^2)†	Total volume of glands (μl)	Total volume of mucous cells (μl)
Trachea	0.0047	0 (Tu)	0.073	0.082	67.86	0.056	0.022
		0 (Tm)	0.087				
		0 (Tl)	0.086				
Primary bronchi	0.0026	1	0.078	0.078	36.49	0.028	0.011
Segmental bronchi	0.0032	2	0.074	0.074	19.82	0.020	0.008
		3	0.052	0.052	10.70		
Distal bronchi	0.0126	4	0.035	0.035	28.73	0.019	0.007
		5	0.017	0.017	26.89		
		6	0.007	0.007	50.67		

*: Values were obtained from reference 65. †: Values were obtained from references 46 and 47. RNA ISH = RNA *in situ* hybridization; SE = superficial epithelium; Tu = upper trachea; Tm = middle trachea; Tl = lower trachea.

Figure 19

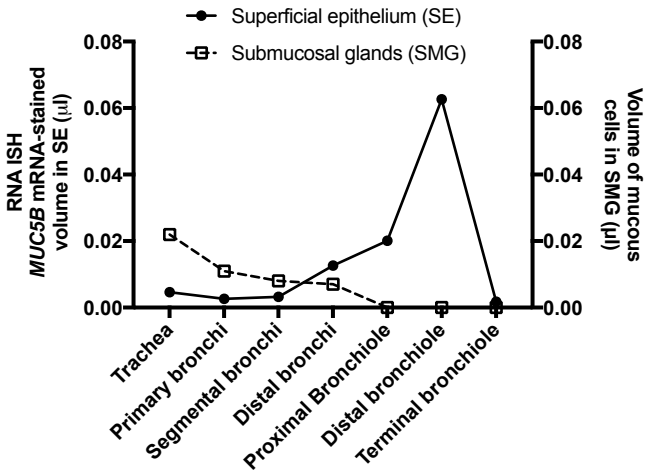

Figure 19. Comparison of superficial epithelial versus submucosal gland sources of MUC5B production in human lungs. Total estimated volumes of mucous cells in normal human submucosal glands (SMG) were compared to RNA ISH-based *MUC5B* mRNA-stained volumes in the histologically normal superficial epithelium (SE) for each airway region. Total volumes of mucous cells in SMG were calculated based on references 65-67.

Interestingly, the SMG and superficial epithelium provide redundant sources for MUC5B in central airway locations. One unresolved issue is whether the superficial epithelium provides the basal MUC5B secretion in this region, as it likely does in mice (17, 18), with SMG providing intermittent secretion to acutely trap inhaled irritants that provoke cough responses. A second unresolved issue with regard to MUC5B biology in the large airways is whether superficial epithelial MUC5B differs from gland-derived MUC5B. Differences may occur because MUC5B appears to be secreted in large airways from different cell types. A CCSP-positive cell without definable granules secretes MUC5B in the superficial epithelium, whereas MUC5B is secreted in SMG from CCSP negative cells with large mucin storage granules. MUC5B is known to exist as two glycoforms with different charges, a low- and a high-charge, and the low-charge MUC5B is elevated in the sputum from the subjects with asthma, CF and COPD (13, 68). Further studies are required to determine whether MUC5B glycan-based charge differs in MUC5B secreted by SMG versus the superficial epithelium.

Our results revealed that neither MUC5B nor MUC5AC is expressed in terminal bronchioles. This finding was also apparent in the group of five subjects with airway GMH (Figure 6B). Interestingly, this finding mimics the absence of Muc5b expression reported in terminal bronchioles of mice (17). Moreover, it is notable that a subtype of *CCSP*+ cells exists in the terminal bronchioles that do not express *MUC5B* but do express *SFTPB* (Figure 16), consistent with previous RNA ISH findings (69). These data are consistent with reports that

SFTPB and mucin gene expression are inversely regulated through NK2 homeobox1 (NKX2-1) at the transcription level (70-72). The finding that secretory mucins are not expressed in terminal bronchioles suggests that the physiology of terminal bronchioles requires a surfactant-rich, mucin-free zone to protect gas exchange functions in alveoli adjacent to terminal bronchioles. Since MUC5B overexpression in peripheral airways is reported in IPF patients and those with rheumatoid arthritis with interstitial lung disease (25-27, 73), it is possible that the loss of a surfactant-rich terminal bronchiolar mucin free zone is a common pathogenesis of interstitial lung disease. Further, in the COPD lung, the distal airway-specific molecular phenotype, including SFTPB expression, was lost in the small airway epithelium and replaced with the proximal airway-specific transcriptomic phenotype such as basal- and mucin-producing cell-related gene expression (60). These findings indicate that restoration of the distal airway-specific molecular features in the small airways can be a fundamental strategy for future therapeutics for muco-obstructive and interstitial lung diseases.

In contrast to MUC5B, which is necessary to sustain MCC (21), MUC5AC has been recognized as a "response mucin" with expression regulated by a number of inflammatory stimuli (5, 16, 34). Our study revealed that MUC5AC-stained volume density peaked at the level of segmental bronchi. Maximal deposition of particles > 1 μm diameter per unit surface area occurs in this region (74), suggesting that MUC5AC is responding to the load of external stimuli deposited in this region. On the other hand, the unique biophysical properties of MUC5AC,

which appear to relate to adhesion and cough clearance, may produce pathological consequences in small airways where MUC5AC-rich mucus is likely to impair MCC (5, 75), suggesting that MUC5AC in small airways can be a potential therapeutic target to restore normal MCC in the muco-obstructive lung diseases. Importantly, it appeared that: 1) MUC5AC expression was superimposed on MUC5B/CCSP expressing cells; and 2) as MUC5AC expression increased, the cell morphology appeared more goblet cell-like.

The RNA ISH approach identified four distinct types of airway secretory cells based on the combination of *MUC5AC*, *MUC5B*, and *CCSP* transcript expression. Each cell-type predominantly exists in different airway regions and SMG versus superficial epithelium (Figure 15). Airway surface secretory epithelial cells have conventionally been divided into four distinct cell types based on morphology and ultrastructure: mucous (goblet), serous, club (Clara), and neuroendocrine cells (76). Mucous cells are mainly located in the tracheobronchial tree and rarely in bronchioles (77). Serous cells have been described in surface epithelium in adult human small bronchi and bronchioles, whereas club cells have been considered to be the predominant secretory cell type in the human bronchiole (78). Juxtaposing these data to our results, CCSP was shown to be expressed not only in typical club cells in distal airways but also non-ciliated airway secretory cells in large airway superficial epithelia. The *CCSP* mRNA+ cells typically expressed *MUC5B*/*MUC5AC* mRNAs in large airway epithelia and *MUC5B* mRNAs in small airway epithelia. Thus, a subset of CCSP+ cells appears to define a

mucin secretory cell type in superficial epithelia.

Consistent with our findings, single cell transcriptome analysis of human airway epithelial club cells revealed that a subset of CCSP+ cells co-expressed MUC5B/MUC5AC, indicating possible lineage relationship between CCSP+ secretory cells and mucin-secreting cells in human airways (79). In contrast, MUC5B-producing cells in SMG may reflect a different lineage because CCSP expression was absent in SMG mucous cells. Morphologically, *CCSP*+/*MUC5B*+/*MUC5AC*- cells in distal airways resembled typical club cells, whereas the morphology of *CCSP*+/*MUC5B*+/*MUC5AC*+ cells in proximal larger airways was variable, reflecting club cells and cells that were termed "mucous cells", "serous cells" or "indeterminate cells" (80, 81). Our data suggest that the current nomenclature of airway secretory cells based on morphologic characteristics may need to be revisited.

Our *in vivo* finding that CCSP+ cells in small airways have the capacity to produce MUC5B was supported by *in vitro* LAE and SAE cell culture data (Figure 17). Interestingly, airway epithelial cells isolated from large and small airway regions were differentiated into phenotypes which maintained region-specific characteristics when cultured under identical conditions. This result recapitulates the previous findings that proximal and distal airway basal cells exhibited region-specific gene expression profiles and progenitor properties during lung regeneration in mice (61, 82).

There are limitations to our morphological studies. First, it is difficult to obtain intact

normal human lungs for studies of regional mucin expression. Although tissues obtained from normal subjects undergoing lung resection for solitary peripheral tumor can be useful for this type of morphometric study, it is still challenging to obtain multiple regions of airways, including tracheas and main bronchi, since these large airways need to be left in the subjects. We adopted the criteria that a histologically normal lung region had to be obtained from a lung donor: 1) without history of lung disease or smoking; 2) exposed to a mechanical ventilation for ≤ 7 days; and 3) did not exhibit GMH as defined by > 0.005 mm^3/mm^2 AB-PAS-stained volume density in a superficial epithelial region, based on the mean value of mucin volume densities in healthy subject group in transbronchial biopsy study (37). Using these criteria, 5 of the 10 lungs from study subjects met the criteria for histologically normal lungs. We speculate that the 5 subjects that exhibited airway GMH were more sensitive to the stresses of the mechanical ventilation, which has been shown to rapidly induce GMH in primary human cell culture models, animal models, and pre-term infants (28, 33-36). If indeed the excluded lungs were histologically normal prior to mechanical ventilation, our data may document how rapidly and substantially large airway GMH can be induced by mechanical stresses (Figure 6B). This notion is also consistent with the localization of NKX2-1 expression, which is shown to inhibit goblet cell metaplasia in distal airways (72). Second, the study group was small, particularly for the RNA ISH and immunohistochemistry studies, due to the strict inclusion criteria used to select histologically normal lungs as described above. Finally, the affinity of

probes for RNA ISH differed for *MUC5AC* and *MUC5B*. Direct measurements of relative RNA ISH *MUC5B* versus *MUC5AC* probe affinities in gene-edited A549 cells, however, provided a useful correction factor. Collectively, the RNA ISH quantitation of *MUC5AC* and *MUC5B*, the absolute mucin transcript expression data by ddPCR in freshly isolated airway surface epithelium, and the cell culture data all agreed that MUC5B is the dominant expressed and secreted mucin in distal human superficial airway epithelia.

In conclusion, MUC5B is extensively expressed in human airway superficial epithelia in addition to SMG. The distal airway region is the major site for MUC5B production in the superficial epithelium of the human lung. MUC5AC is normally only produced by the superficial epithelia of the cartilaginous larger airways. Both MUC5B and MUC5AC are co-localized in CCSP+ cells in proximal superficial epithelium, whereas MUC5B is co-localized in CCSP+ cells of distal airway superficial epithelia. Our study suggests an important property in mucin secretion of the superficial epithelium in the distal airways that are the initial site of mucus plugging in muco-obstructive and possibly IPF diseases.

Reprinted with permission of the American Thoracic Society. Copyright © 2019 American Thoracic Society.

Cite: Kenichi Okuda, Gang Chen, Durai B. Subramani, Monroe Wolf, Rodney C. Gilmore, Takafumi Kato, Giorgia Radicioni, Mehmet Kesimer, Michael Chua, Hong Dang, Alessandra

Livraghi-Butrico, Camille Ehre, Claire M. Doerschuk, Scott H. Randell, Hirotoshi Matsui, Takahide Nagase, Wanda K. O'Neal and Richard C. Boucher/ 2019/ Localization of Secretory Mucins MUC5AC and MUC5B in Normal/Healthy Human Airways/ American Journal of Respiratory and Critical Care Medicine/ Volume 199/ Issue 6/ Pages 715-727.

The *American Journal of Respiratory and Critical Care Medicine* is an official journal of the American Thoracic Society.

7. Acknowledgments

I would like to express my sincere gratitude to Prof. Takahide Nagase and Prof. Richard C. Boucher for their supervision to accomplish this study. I am deeply grateful to Dr. Wanda K. O'Neal, Dr. Gang Chen and Dr. Hirotoshi Matsui for providing the guidance and feedback to the overall work. I also appreciate Dr. Scott H. Randell for providing human lung samples and Dr. Claire M. Doerschuk for histopathological analysis. Finally, I would like to express my gratitude to Dr. Camille Ehre, Dr. Alessandra Livraghi-Butrico, Dr. Hong Dang, Dr. Michael Chua, Dr. Mehmet Kesimer, Dr. Giorgia Radicioni, Dr. Durai B. Subramani, Dr. Takafumi Kato, Rodney C. Gilmore, and Monroe Wolf for providing technical advice and assistance for this study.

8. References

1. Ghosh A, Boucher RC, Tarran R. Airway hydration and COPD. *Cellular and molecular life sciences : CMLS* 2015; 72: 3637-3652.

2. Burgel PR, Montani D, Danel C, Dusser DJ, Nadel JA. A morphometric study of mucins and small airway plugging in cystic fibrosis. *Thorax* 2007; 62: 153-161.

3. Groneberg DA, Eynott PR, Oates T, Lim S, Wu R, Carlstedt I, Nicholson AG, Chung KF. Expression of MUC5AC and MUC5B mucins in normal and cystic fibrosis lung. *Respiratory medicine* 2002; 96: 81-86.

4. Kirkham S, Kolsum U, Rousseau K, Singh D, Vestbo J, Thornton DJ. MUC5B is the major mucin in the gel phase of sputum in chronic obstructive pulmonary disease. *American journal of respiratory and critical care medicine* 2008; 178: 1033-1039.

5. Bonser LR, Zlock L, Finkbeiner W, Erle DJ. Epithelial tethering of MUC5AC-rich mucus impairs mucociliary transport in asthma. *The Journal of Clinical Investigation* 2016.

6. Groneberg DA, Eynott PR, Lim S, Oates T, Wu R, Carlstedt I, Roberts P, McCann B, Nicholson AG, Harrison BD, Chung KF. Expression of respiratory mucins in fatal status asthmaticus and mild asthma. *Histopathology* 2002; 40: 367-373.

7. Button B, Cai LH, Ehre C, Kesimer M, Hill DB, Sheehan JK, Boucher RC, Rubinstein M. A periciliary brush promotes the lung health by separating the mucus layer from airway epithelia. *Science* 2012; 337: 937-941.

8. Kesimer M, Ehre C, Burns KA, Davis CW, Sheehan JK, Pickles RJ. Molecular organization of the mucins and glycocalyx underlying mucus transport over mucosal surfaces of the airways. *Mucosal immunology* 2013; 6: 379-392.

9. Anderson WH, Coakley RD, Button B, Henderson AG, Zeman KL, Alexis NE, Peden DB, Lazarowski ER, Davis CW, Bailey S, Fuller F, Almond M, Qaqish B, Bordonali E, Rubinstein M, Bennett WD, Kesimer M, Boucher RC. The Relationship of Mucus Concentration (Hydration) to Mucus Osmotic Pressure and Transport in Chronic Bronchitis. *American journal of respiratory and critical care medicine* 2015; 192: 182-190.

10. Henderson AG, Ehre C, Button B, Abdullah LH, Cai LH, Leigh MW, DeMaria GC, Matsui H, Donaldson SH, Davis CW, Sheehan JK, Boucher RC, Kesimer M. Cystic fibrosis airway secretions exhibit mucin hyperconcentration and increased osmotic pressure. *The Journal of Clinical Investigation* 2014; 124: 3047-3060.

11. Kesimer M, Kirkham S, Pickles RJ, Henderson AG, Alexis NE, Demaria G, Knight D, Thornton DJ, Sheehan JK. Tracheobronchial air-liquid interface cell culture: a model for innate mucosal defense of the upper airways? *American journal of physiology Lung cellular and molecular physiology* 2009; 296: L92-l100.

12. Buisine MP, Devisme L, Copin MC, Durand-Reville M, Gosselin B, Aubert JP, Porchet N. Developmental mucin gene expression in the human respiratory tract. *American journal of respiratory cell and molecular biology* 1999; 20: 209-218.

13. Kirkham S, Sheehan JK, Knight D, Richardson PS, Thornton DJ. Heterogeneity of airways mucus: variations in the amounts and glycoforms of the major oligomeric mucins MUC5AC and MUC5B. *The Biochemical journal* 2002; 361: 537-546.

14. Audie JP, Janin A, Porchet N, Copin MC, Gosselin B, Aubert JP. Expression of human mucin genes in respiratory, digestive, and reproductive tracts ascertained by in situ hybridization. *J Histochem Cytochem* 1993; 41: 1479-1485.

15. Hovenberg HW, Davies JR, Carlstedt I. Different mucins are produced by the surface epithelium and the submucosa in human trachea: identification of MUC5AC as a major mucin from the goblet cells. *The Biochemical journal* 1996; 318 (Pt 1): 319-324.

16. Young HW, Williams OW, Chandra D, Bellinghausen LK, Perez G, Suarez A, Tuvim MJ, Roy MG, Alexander SN, Moghaddam SJ, Adachi R, Blackburn MR, Dickey BF, Evans CM. Central role of Muc5ac expression in mucous metaplasia and its regulation by conserved 5' elements. *American journal of respiratory cell and molecular biology* 2007; 37: 273-290.

17. Zhu Y, Ehre C, Abdullah LH, Sheehan JK, Roy M, Evans CM, Dickey BF, Davis CW. Munc13-2-/- baseline secretion defect reveals source of oligomeric mucins in mouse airways. *The Journal of physiology* 2008; 586: 1977-1992.

18. Davis CW, Dickey BF. Regulated airway goblet cell mucin secretion. *Annual review of physiology* 2008; 70: 487-512.

19. Fahy JV, Dickey BF. Airway Mucus Function and Dysfunction. *New England Journal of Medicine* 2010; 363: 2233-2247.

20. Evans CM, Williams OW, Tuvim MJ, Nigam R, Mixides GP, Blackburn MR, DeMayo FJ, Burns AR, Smith C, Reynolds SD, Stripp BR, Dickey BF. Mucin is produced by clara cells in the proximal airways of antigen-challenged mice. *American journal of respiratory cell and molecular biology* 2004; 31: 382-394.

21. Roy MG, Livraghi-Butrico A, Fletcher AA, McElwee MM, Evans SE, Boerner RM, Alexander SN, Bellinghausen LK, Song AS, Petrova YM, Tuvim MJ, Adachi R, Romo I, Bordt AS, Bowden MG, Sisson JH, Woodruff PG, Thornton DJ, Rousseau K, De la Garza MM, Moghaddam SJ, Karmouty-Quintana H, Blackburn MR, Drouin SM, Davis CW, Terrell KA, Grubb BR, O'Neal WK, Flores SC, Cota-Gomez A, Lozupone CA, Donnelly JM, Watson AM, Hennessy CE, Keith RC, Yang IV, Barthel L, Henson PM, Janssen WJ, Schwartz DA, Boucher RC, Dickey BF, Evans CM. Muc5b is required for airway defence. *Nature* 2014; 505: 412-416.

22. Rock JR, Randell SH, Hogan BL. Airway basal stem cells: a perspective on their roles in epithelial homeostasis and remodeling. *Disease models & mechanisms* 2010; 3: 545-556.

23. Caramori G, Di Gregorio C, Carlstedt I, Casolari P, Guzzinati I, Adcock IM, Barnes PJ, Ciaccia A, Cavallesco G, Chung KF, Papi A. Mucin expression in peripheral airways of patients with chronic obstructive pulmonary disease. *Histopathology* 2004; 45: 477-484.

24. Casalino-Matsuda SM, Monzon ME, Day AJ, Forteza RM. Hyaluronan fragments/CD44 mediate oxidative stress-induced MUC5B up-regulation in airway epithelium. *American journal of respiratory cell and molecular biology* 2009; 40: 277-285.

25. Seibold MA, Smith RW, Urbanek C, Groshong SD, Cosgrove GP, Brown KK, Schwarz MI, Schwartz DA, Reynolds SD. The Idiopathic Pulmonary Fibrosis Honeycomb Cyst Contains A Mucocilary Pseudostratified Epithelium. *PloS one* 2013; 8: e58658.

26. Nakano Y, Yang IV, Walts AD, Watson AM, Helling BA, Fletcher AA, Lara AR, Schwarz MI, Evans CM, Schwartz DA. MUC5B Promoter Variant rs35705950 Affects MUC5B Expression in the Distal Airways in Idiopathic Pulmonary Fibrosis. *American journal of respiratory and critical care medicine* 2016; 193: 464-466.

27. Conti C, Montero-Fernandez A, Borg E, Osadolor T, Viola P, De Lauretis A, Stock CJ, Bonifazi M, Bonini M, Caramori G, Lindahl G, Blasi FB, Nicholson AG, Wells AU,

Sestini P, Renzoni E. Mucins MUC5B and MUC5AC in Distal Airways and Honeycomb Spaces: Comparison among Idiopathic Pulmonary Fibrosis/Usual Interstitial Pneumonia, Fibrotic Nonspecific Interstitial Pneumonitis, and Control Lungs. *American journal of respiratory and critical care medicine* 2016; 193: 462-464.

28. Deputla N, Royse E, Kemp MW, Miura Y, Kallapur SG, Jobe AH, Hillman NH. Brief mechanical ventilation causes differential epithelial repair along the airways of fetal, preterm lambs. *American journal of physiology Lung cellular and molecular physiology* 2016: ajplung 00181 02016.

29. Innes AL, Woodruff PG, Ferrando RE, Donnelly S, Dolganov GM, Lazarus SC, Fahy JV. Epithelial mucin stores are increased in the large airways of smokers with airflow obstruction. *Chest* 2006; 130: 1102-1108.

30. Okuda K, Chen G, Subramani DB, Wolf M, Gilmore RC, Kato T, Radicioni G, Kesimer M, Chua M, Dang H, Livraghi-Butrico A, Ehre C, Doerschuk CM, Randell SH, Matsui H, Nagase T, O'Neal WK, Boucher RC. Localization of Secretory Mucins MUC5AC and MUC5B in Normal/Healthy Human Airways. *American journal of respiratory and critical care medicine* 2018.

31. Van Raemdonck D, Neyrinck A, Verleden GM, Dupont L, Coosemans W, Decaluwe H, Decker G, De Leyn P, Nafteux P, Lerut T. Lung donor selection and management. *Proceedings of the American Thoracic Society* 2009; 6: 28-38.

32. Seibold MA, Wise AL, Speer MC, Steele MP, Brown KK, Loyd JE, Fingerlin TE, Zhang W, Gudmundsson G, Groshong SD, Evans CM, Garantziotis S, Adler KB, Dickey BF, du Bois RM, Yang IV, Herron A, Kervitsky D, Talbert JL, Markin C, Park J, Crews AL, Slifer SH, Auerbach S, Roy MG, Lin J, Hennessy CE, Schwarz MI, Schwartz DA. A common MUC5B promoter polymorphism and pulmonary fibrosis. *The New England journal of medicine* 2011; 364: 1503-1512.

33. Hislop AA, Haworth SG. Airway size and structure in the normal fetal and infant lung and the effect of premature delivery and artificial ventilation. *Am Rev Respir Dis* 1989; 140: 1717-1726.

34. Park JA, Tschumperlin DJ. Chronic intermittent mechanical stress increases MUC5AC protein expression. *American journal of respiratory cell and molecular biology* 2009; 41: 459-466.

35. Hillman NH, Moss TJ, Kallapur SG, Bachurski C, Pillow JJ, Polglase GR, Nitsos I, Kramer BW, Jobe AH. Brief, large tidal volume ventilation initiates lung injury and a systemic response in fetal sheep. *American journal of respiratory and critical care medicine* 2007; 176: 575-581.

36. Koeppen M, McNamee EN, Brodsky KS, Aherne CM, Faigle M, Downey GP, Colgan SP, Evans CM, Schwartz DA, Eltzschig HK. Detrimental role of the airway mucin Muc5ac during ventilator-induced lung injury. *Mucosal immunology* 2013; 6: 762-775.

37. OrdoÑEz CL, Khashayar R, Wong HH, Ferrando RON, Wu R, Hyde DM, Hotchkiss JA, Zhang Y, Novikov A, Dolganov G, Fahy JV. Mild and Moderate Asthma Is Associated with Airway Goblet Cell Hyperplasia and Abnormalities in Mucin Gene Expression. *American journal of respiratory and critical care medicine* 2001; 163: 517-523.

38. Wright JL, Lawson LM, Pare PD, Wiggs BJ, Kennedy S, Hogg JC. Morphology of peripheral airways in current smokers and ex-smokers. *Am Rev Respir Dis* 1983; 127: 474-477.

39. Soderberg M, Hellstrom S, Sandstrom T, Lundgren R, Bergh A. Structural characterization of bronchial mucosal biopsies from healthy volunteers: a light and electron microscopical study. *Eur Respir J* 1990; 3: 261-266.

40. Li X, Tang XX, Vargas Buonfiglio LG, Comellas AP, Thornell IM, Ramachandran S, Karp PH, Taft PJ, Sheets K, Abou Alaiwa MH, Welsh MJ, Meyerholz DK, Stoltz DA, Zabner J. Electrolyte transport properties in distal small airways from cystic fibrosis

pigs with implications for host defense. *American journal of physiology Lung cellular and molecular physiology* 2016; 310: L670-679.

41. Gentzsch M, Boyles SE, Cheluvaraju C, Chaudhry IG, Quinney NL, Cho C, Dang H, Liu X, Schlegel R, Randell SH. Pharmacological Rescue of Conditionally Reprogrammed Cystic Fibrosis Bronchial Epithelial Cells. *American journal of respiratory cell and molecular biology* 2016.

42. Mullen JB, Wright JL, Wiggs BR, Pare PD, Hogg JC. Structure of central airways in current smokers and ex-smokers with and without mucus hypersecretion: relationship to lung function. *Thorax* 1987; 42: 843-848.

43. Kim S, Shim JJ, Burgel PR, Ueki IF, Dao-Pick T, Tam DC, Nadel JA. IL-13-induced Clara cell secretory protein expression in airway epithelium: role of EGFR signaling pathway. *American journal of physiology Lung cellular and molecular physiology* 2002; 283: L67-75.

44. Kim V, Oros M, Durra H, Kelsen S, Aksoy M, Cornwell WD, Rogers TJ, Criner GJ. Chronic Bronchitis and Current Smoking Are Associated with More Goblet Cells in Moderate to Severe COPD and Smokers without Airflow Obstruction. *PloS one* 2015; 10: e0116108.

45. Kim V, Kelemen SE, Abuel-Haija M, Gaughan JP, Sharafkaneh A, Evans CM, Dickey BF, Solomides CC, Rogers TJ, Criner GJ. Small airway mucous metaplasia and inflammation in chronic obstructive pulmonary disease. *COPD* 2008; 5: 329-338.

46. Wiggs BR, Moreno R, Hogg JC, Hilliam C, Pare PD. A model of the mechanics of airway narrowing. *Journal of applied physiology (Bethesda, Md : 1985)* 1990; 69: 849-860.

47. Weibel ER. Chapter XI - Geometric and Dimensional Airway Models of Conductive, Transitory and Respiratory Zones of the Human Lung. Morphometry of the Human Lung: Academic Press; 1963. p. 136-142.

48. Fulcher ML, Gabriel S, Burns KA, Yankaskas JR, Randell SH. Well-differentiated human airway epithelial cell cultures. *Methods in molecular medicine* 2005; 107: 183-206.

49. Abdullah LH, Coakley R, Webster MJ, Zhu Y, Tarran R, Radicioni G, Kesimer M, Boucher RC, Davis CW, Ribeiro CMP. Mucin Production and Hydration Responses to Mucopurulent Materials in Normal vs. CF Airway Epithelia. *American journal of respiratory and critical care medicine* 2017.

50. Livraghi-Butrico A, Grubb BR, Wilkinson KJ, Volmer AS, Burns KA, Evans CM, O'Neal WK, Boucher RC. Contribution of mucus concentration and secreted mucins Muc5ac and Muc5b to the pathogenesis of muco-obstructive lung disease. *Mucosal immunology* 2016.

51. McDermott GP, Do D, Litterst CM, Maar D, Hindson CM, Steenblock ER, Legler TC, Jouvenot Y, Marrs SH, Bemis A, Shah P, Wong J, Wang S, Sally D, Javier L, Dinio T, Han C, Brackbill TP, Hodges SP, Ling Y, Klitgord N, Carman GJ, Berman JR, Koehler RT, Hiddessen AL, Walse P, Bousse L, Tzonev S, Hefner E, Hindson BJ, Cauly TH, 3rd, Hamby K, Patel VP, Regan JF, Wyatt PW, Karlin-Neumann GA, Stumbo DP, Lowe AJ. Multiplexed target detection using DNA-binding dye chemistry in droplet digital PCR. *Analytical chemistry* 2013; 85: 11619-11627.

52. Stauber J, Shaikh N, Ordiz MI, Tarr PI, Manary MJ. Droplet digital PCR quantifies host inflammatory transcripts in feces reliably and reproducibly. *Cellular immunology* 2016; 303: 43-49.

53. Sacher AG, Paweletz C, Dahlberg SE, Alden RS, O'Connell A, Feeney N, Mach SL, Janne PA, Oxnard GR. Prospective Validation of Rapid Plasma Genotyping for the Detection of EGFR and KRAS Mutations in Advanced Lung Cancer. *JAMA oncology* 2016; 2: 1014-1022.

54. Kesimer M, Cullen J, Cao R, Radicioni G, Mathews KG, Seiler G, Gookin JL. Excess Secretion of Gel-Forming Mucins and Associated Innate Defense Proteins with Defective Mucin Un-Packaging Underpin Gallbladder Mucocele Formation in Dogs. *PloS one* 2015; 10: e0138988.

55. Kesimer M, Ford AA, Ceppe A, Radicioni G, Cao R, Davis CW, Doerschuk CM, Alexis NE, Anderson WH, Henderson AG, Barr RG, Bleecker ER, Christenson SA, Cooper CB, Han MK, Hansel NN, Hastie AT, Hoffman EA, Kanner RE, Martinez F, Paine RI, Woodruff PG, O'Neal WK, Boucher RC. Airway Mucin Concentration as a Marker of Chronic Bronchitis. *New England Journal of Medicine* 2017; 377: 911-922.

56. Sanjana NE, Shalem O, Zhang F. Improved vectors and genome-wide libraries for CRISPR screening. *Nat Methods* 2014; 11: 783-784.

57. Subramani DB, Sears PR, Hill DB, Button B, Rubinstein MR, Kesimer M, Ostrowski LE, O'Neal W, Boucher RC. Why two mucins (MUC5B and MUC5AC) in cystic fibrosis [abstract]. Pediatric Pulmonology 2016; 51: S252.

58. OrdoÑEz CL, Khashayar R, Wong HH, Ferrando RON, Wu R, Hyde DM, Hotchkiss JA, Zhang Y, Novikov A, Dolganov G, Fahy JV. Mild and Moderate Asthma Is Associated with Airway Goblet Cell Hyperplasia and Abnormalities in Mucin Gene Expression. *American journal of respiratory and critical care medicine* 2001; 163: 517-523.

59. Chen G, Korfhagen TR, Karp CL, Impey S, Xu Y, Randell SH, Kitzmiller J, Maeda Y, Haitchi HM, Sridharan A, Senft AP, Whitsett JA. Foxa3 induces goblet cell metaplasia and inhibits innate antiviral immunity. *American journal of respiratory and critical care medicine* 2014; 189: 301-313.

60. Yang J, Zuo WL, Fukui T, Chao I, Gomi K, Lee B, Staudt MR, Kaner RJ, Strulovici-Barel Y, Salit J, Crystal RG, Shaykhiev R. Smoking-dependent Distal-to-Proximal Repatterning of the Adult Human Small Airway Epithelium. *American journal of respiratory and critical care medicine* 2017.

61. Kumar PA, Hu Y, Yamamoto Y, Hoe NB, Wei TS, Mu D, Sun Y, Joo LS, Dagher R, Zielonka EM, Wang de Y, Lim B, Chow VT, Crum CP, Xian W, McKeon F. Distal airway stem cells yield alveoli in vitro and during lung regeneration following H1N1 influenza infection. *Cell* 2011; 147: 525-538.

62. Crystal RG, Randell SH, Engelhardt JF, Voynow J, Sunday ME. Airway epithelial cells: current concepts and challenges. *Proceedings of the American Thoracic Society* 2008; 5: 772-777.

63. Hogan BL, Barkauskas CE, Chapman HA, Epstein JA, Jain R, Hsia CC, Niklason L, Calle E, Le A, Randell SH, Rock J, Snitow M, Krummel M, Stripp BR, Vu T, White ES, Whitsett JA, Morrisey EE. Repair and regeneration of the respiratory system: complexity, plasticity, and mechanisms of lung stem cell function. *Cell stem cell* 2014; 15: 123-138.

64. Hackett NR, Butler MW, Shaykhiev R, Salit J, Omberg L, Rodriguez-Flores JL, Mezey JG, Strulovici-Barel Y, Wang G, Didon L, Crystal RG. RNA-Seq quantification of the human small airway epithelium transcriptome. *BMC genomics* 2012; 13: 82.

65. Whimster WF. Tracheobronchial submucous gland profiles in smokers and non-smokers. *Appl Pathol* 1988; 6: 241-246.

66. Basbaum CB, Jany B, Finkbeiner WE. The serous cell. *Annual review of physiology* 1990; 52: 97-113.

67. Takizawa T, Thurlbeck WM. A comparative study of four methods of assessing the morphologic changes in chronic bronchitis. *Am Rev Respir Dis* 1971; 103: 774-783.

68. Welsh KG, Rousseau K, Fisher G, Bonser LR, Bradding P, Brightling CE, Thornton DJ, Gaillard EA. MUC5AC and a Glycosylated Variant of MUC5B Alter Mucin Composition in Children With Acute Asthma. *Chest* 2017.

69. Phelps DS, Floros J. Localization of surfactant protein synthesis in human lung by in situ hybridization. *Am Rev Respir Dis* 1988; 137: 939-942.

70. Attarian SJ, Leibel SL, Yang P, Alfano DN, Hackett BP, Cole FS, Hamvas A. Mutations in the thyroid transcription factor gene NKX2-1 result in decreased expression of SFTPB and SFTPC. *Pediatric research* 2018.

71. Guo M, Tomoshige K, Meister M, Muley T, Fukazawa T, Tsuchiya T, Karns R, Warth A, Fink-Baldauf IM, Nagayasu T, Naomoto Y, Xu Y, Mall MA, Maeda Y. Gene signature driving invasive mucinous adenocarcinoma of the lung. *EMBO molecular medicine* 2017; 9: 462-481.

72. Maeda Y, Chen G, Xu Y, Haitchi HM, Du L, Keiser AR, Howarth PH, Davies DE, Holgate ST, Whitsett JA. Airway epithelial transcription factor NK2 homeobox 1 inhibits mucous cell metaplasia and Th2 inflammation. *American journal of respiratory and critical care medicine* 2011; 184: 421-429.

73. Juge PA, Lee JS, Ebstein E, Furukawa H, Dobrinskikh E, Gazal S, Kannengiesser C, Ottaviani S, Oka S, Tohma S, Tsuchiya N, Rojas-Serrano J, Gonzalez-Perez MI, Mejia M, Buendia-Roldan I, Falfan-Valencia R, Ambrocio-Ortiz E, Manali E, Papiris SA, Karageorgas T, Boumpas D, Antoniou K, van Moorsel CHM, van der Vis J, de Man YA, Grutters JC, Wang Y, Borie R, Wemeau-Stervinou L, Wallaert B, Flipo RM, Nunes H, Valeyre D, Saidenberg-Kermanac'h N, Boissier MC, Marchand-Adam S, Frazier A, Richette P, Allanore Y, Sibilia J, Dromer C, Richez C, Schaeverbeke T, Liote H, Thabut G, Nathan N, Amselem S, Soubrier M, Cottin V, Clement A, Deane K, Walts AD, Fingerlin T, Fischer A, Ryu JH, Matteson EL, Niewold TB, Assayag D, Gross A, Wolters P, Schwarz MI, Holers M, Solomon J, Doyle T, Rosas IO, Blauwendraat C, Nalls MA, Debray MP, Boileau C, Crestani B, Schwartz DA, Dieude P. MUC5B Promoter Variant and Rheumatoid Arthritis with Interstitial Lung Disease. *The New England journal of medicine* 2018.

74. Gerrity TR, Lee PS, Hass FJ, Marinelli A, Werner P, Lourenco RV. Calculated deposition of inhaled particles in the airway generations of normal subjects. *J Appl Physiol Respir Environ Exerc Physiol* 1979; 47: 867-873.

75. Button B, Goodell HP, Atieh E, Chen Y-C, Williams R, Shenoy S, Lackey E, Shenkute NT, Cai L-H, Dennis RG, Boucher RC, Rubinstein M. Roles of mucus adhesion and cohesion in cough clearance. *Proceedings of the National Academy of Sciences* 2018.

76. Jeffery PK, Li D. Airway mucosa: secretory cells, mucus and mucin genes. *Eur Respir J* 1997; 10: 1655-1662.

77. Lumsden AB, McLean A, Lamb D. Goblet and Clara cells of human distal airways: evidence for smoking induced changes in their numbers. *Thorax* 1984; 39: 844-849.

78. Rogers AV, Dewar A, Corrin B, Jeffery PK. Identification of serous-like cells in the surface epithelium of human bronchioles. *Eur Respir J* 1993; 6: 498-504.

79. Zuo WL, Shenoy SA, Li S, O'Beirne SL, Strulovici-Barel Y, Leopold PL, Wang G, Staudt MR, Walters MS, Mason C, Kaner RJ, Mezey JG, Crystal RG. Ontogeny and Biology of Human Small Airway Epithelial Club Cells. *American journal of respiratory and critical care medicine* 2018.

80. Boers JE, Ambergen AW, Thunnissen FB. Number and proliferation of clara cells in normal human airway epithelium. *American journal of respiratory and critical care medicine* 1999; 159: 1585-1591.

81. Jeffery PK, Gaillard D, Moret S. Human airway secretory cells during development and in mature airway epithelium. *Eur Respir J* 1992; 5: 93-104.

82. Zuo W, Zhang T, Wu DZ, Guan SP, Liew AA, Yamamoto Y, Wang X, Lim SJ, Vincent M, Lessard M, Crum CP, Xian W, McKeon F. p63(+)Krt5(+) distal airway stem cells are essential for lung regeneration. *Nature* 2015; 517: 616-620.